Supplementary Information (SI) for Chemical Science.
This journal is © The Royal Society of Chemistry 2024

Electronic Supporting Information

Deciphering charge transfer dynamics of lead halide perovskite-nickel(II) complex for visible light photoredox C–N coupling

Vishesh Kumar,[a] Sunil Kumar Patel,[b] Ved Vyas,[a] Deepak Kumar,[a] E. Siva Subramaniam Iyer,[b*] and Arindam Indra[a*]

[a] Department of Chemistry, Indian Institute of Technology (BHU), Varanasi, UP-221005, India
E-mail: arindam.chy@iitbhu.ac.in
[b] School of Chemical and Materials Sciences, Indian Institute of Technology Goa, Ponda, Goa, India.
Email: essiyer@iitgoa.ac.in

Chemicals

Lead(II) bromide (99.9%), oleic acid (OA, 90%), 1-octadecene (ODE, 91%), and tetrabutylammonium hexafluorophosphate ($TBHPF_6$) were purchased from Sigma-Aldrich. Nickel(II) chloride hexahydrate was purchased from SD Fine-Chemical Limited. Ethyl acetate (99.9%), sodium hydroxide, dimethylglyoxime ($dmgH_2$), cesium carbonate (99.9%), oleylamine (OAm, 90%), and anhydrous solvents like tetrahydrofuran, toluene, acetonitrile were purchased from Sisco Research Laboratories Pvt. Ltd, India. *P*-Nitro-Blue tetrazolium chloride (NBT) and *o*-Tolidine were purchased from Sigma-Aldrich. Chloroform-d ($CDCl_3$), hexane, and silica gel were purchased from Merck. All aldehydes and amine substrates were purchased from either Sigma-Aldrich, SRL, or Merck.

Instrumental

The PXRD data were acquired within 2θ range of 5-80° using a Rigaku D/MAX RINT-2000 X-Ray diffractometer, with Cu-K_α (λ = 1.5418Å) radiation.

The X-ray photoelectron spectroscopy (XPS) was conducted on a VG/VG ESCA LAB 220i X-ray photoelectron spectrometer. The acquired XPS was deconvoluted and analyzed using Origin 8.5 software. Diffuse reflectance spectroscopy (DRS) measurements using UV-Vis were conducted utilizing an AvaSpec-ULS2048L instrument. Photoluminescence spectra were recorded on a TCSPC system from Horiba Yovin (Delta Flex).

Transmission electron microscopy (TEM) analyses were conducted using an FEI Tecnai G2 20 S-TWIN instrument equipped with an energy-dispersive X-ray spectrometer (EDAX, r-TEM SUTW).

^{1}H-NMR and ^{13}C-NMR spectra were recorded on AVH D 500 AVANCE III HD 500 MHz One Bay NMR Spectrometer from Bruker Bio Spin International and Advance Neo 600 MHz Bruker India Scientific. The chemical shifts and coupling constants were reported in ppm. The abbreviations used are as follows: "s" for singlet, "bs" for broad singlet, "d" for doublet, "t" for triplet, and "m" for multiple. Residual solvent signals ($CDCl_3$: δ_H = 7.28-7.29 ppm and δ_C = 77.01-77.16 ppm) were used as the references for ^{1}H and ^{13}C NMR spectra, respectively.

HRMS (m/z) were recorded in an electron ionization or electrospray ionization (ESI) mode on Waters-Q-TOF Premier-HAB213 and Sciex X500R QTOF instruments.

Light source for the photocatalytic reaction: (JACKAL, LED 3-Watt blue light, 460±5 nm). 5 Lights were used together.

Experimental Section

Synthesis of $CsPbBr_3$

The $CsPbBr_3$ quantum dots (QDs) were synthesized by following a previously reported method with modifications.[1] Cs_2CO_3 (130.3 mg, 0.4 mmol), ODE (6 mL), and OA (0.5 mL) were taken in a 250 mL 3-neck round bottom flask, which was then heated for 1 hour at 120 °C in N_2, it was further heated at 150 °C for 10 minutes until the Cs_2CO_3 was completely dissolved to form Cs-oleate. Cs-oleate precursor solution was kept at 100 °C.

In a 3-neck round bottom flask, $PbBr_2$ (73 mg, 0.2 mmol) and ODE (10 mL) were stirred for one hour at 120 °C under vacuum. Next, the atmosphere was changed to N_2, and dried OA and OAm (0.5 mL each) were added to the above solution. The temperature of the solution was increased to 170 °C to make it completely soluble. The Cs-oleate solution (0.4 mL) was then rapidly injected into the mixture solution and stirred for 5 seconds. The crude mixture was immediately cooled down by immersing the round bottom flask in an ice-water bath. The precipitate was centrifuged at different rpm and washed with ethyl acetate. Further, the yellow precipitate of $CsPbBr_3$ was vacuum-dried.

Synthesis of Nickel(II) dimethylglyoxime [$Ni(dmgH)_2$] complex

$Ni(dmgH)_2$ was prepared using a known procedure.[2] A solution of dimethylglyoxime (2.2 mmol) in ethanol (20 mL) was added to an aqueous solution of $NiCl_2.6H_2O$ (1 mmol) and the whole mixture was made alkaline (pH = 9) with aqueous ammonia. After stirring for 15 min, the resulting mixture was filtered, and washed with ethanol and distilled water. The residue was dried for 12 h at 60 °C.

The salen ligands were synthesized according to a method reported in the literature.[3,4] Similarly, a previously reported process Ni(II)–salen complex was synthesized.[5]

Preparation of standard wt.% [Ni]-$CsPbBr_3$

93 mg $CsPbBr_3$ QDs were re-dispersed in THF (7 mL). 7 mg $Ni(dmgH)_2$ was dispersed in 3 mL (THF) solution added into $CsPbBr_3$ solution and stirred in the dark for 10 min to make a homogeneous solution, denoted to 7% [Ni]-$CsPbBr_3$. Further, pipette out 1 mL of catalyst solution for every reaction.

For the solid-state characterization, 7% [Ni]-$CsPbBr_3$ solid sample was obtained by vacuum drying. Similarly, different wt.% of cocatalysts were loaded as listed in Table S1.

Table S1. Description of the photocatalyst systems.

S.N.	Photocatalyst	Cocatalyst	Loading (wt.%)	Code
1	$CsPbBr_3$	$Ni(dmgH)_2$	0	$CsPbBr_3$
2	$CsPbBr_3$	$Ni(dmgH)_2$	3	3% [Ni]-$CsPbBr_3$
3	$CsPbBr_3$	$Ni(dmgH)_2$	5	5% [Ni]-$CsPbBr_3$
4	$CsPbBr_3$	$Ni(dmgH)_2$	7	7% [Ni]-$CsPbBr_3$
5	$CsPbBr_3$	$Ni(dmgH)_2$	9	9% [Ni]-$CsPbBr_3$

Photocatalytic activity Test

The C–N coupling of aldehyde and amine was carried out in a 15 mL quartz vial associated with a water circulation system. 0.5 mmol aldehyde and 1 mmol amine were taken in 2 ml THF. To this solution, photocatalyst solution in THF (1.0 mL, contains 10 mg photocatalyst) was added and the reaction mixture was stirred in the dark for 10 minutes to make a homogeneous solution and to ensure the adsorption-desorption equilibrium between the catalyst and substrates. The vial was placed 8 cm away from the light and irradiated for 18 h with stirring (400 rpm). The reaction temperature was maintained 35±3 ^{o}C. After the completion of the reaction, the mixture was centrifuged (15000 rpm for 10 minutes) to separate the photocatalyst. The liquid part was collected and worked up. The isolated product yield was reported while the product was characterized by ^{1}H and ^{13}C NMR. After each amination test, the catalyst was washed with ethanol, separated by centrifugation several times, and vacuum-dried overnight for the recycling test.

Working electrode preparation

3 mg catalyst was sonicated for 10 minutes in 1 mL ethyl acetate. Further, 300 µL mixture was dropped casted on FTO (geometrical surface area of 1x1 cm^2) and dried for 30 minutes at 50 ^{o}C.

Photoelectrochemical measurements

Photoelectrochemical investigations were conducted using a Metrohm Auto Lab M204 workstation with 15 W Blue LED. The experimental setup featured a Pt wire as the counter electrode, Ag/AgCl as the reference electrode, and the working electrode comprising of fluorine-doped tin oxide (FTO) loaded with catalyst. 0.1 M tetrabutylammonium hexafluorophosphate ($TBAPF_6$) in ethyl acetate was used as the electrolyte.

Ultrafast transient absorption

The ultrafast Transient Absorption (TA) experimental arrangement utilized an 80 MHz mode-locked laser.

The samples were kept in a sealed quartz cuvette with a path length of 2 mm. The samples used in the experiments were suspended in THF and the OD was maintained ~0.4 in 2 mm path length. The sample was stirred using a magnetic stirrer. The pump wavelength of 370 nm (10 nJ) was generated from Operasolo OPA. A White light probe was generated by focusing a segment of the amplified output center at 800 nm by an Astrella amplifier from Coherent USA operating at 1 kHz on a CaF_2 Crystal. The white light was split using a beam splitter to generate both signal and reference beams. These beams were directed through a fiber coupling unit to the detector (photodiode detector array) to capture the pump-induced changes at various delay times of the probe beam. All spectra were chirp corrected and

measurement was conducted delay time window of up to 6 ns. The TA spectra are analyzed using Surface Explorer, V.4.2 software.

Figures:

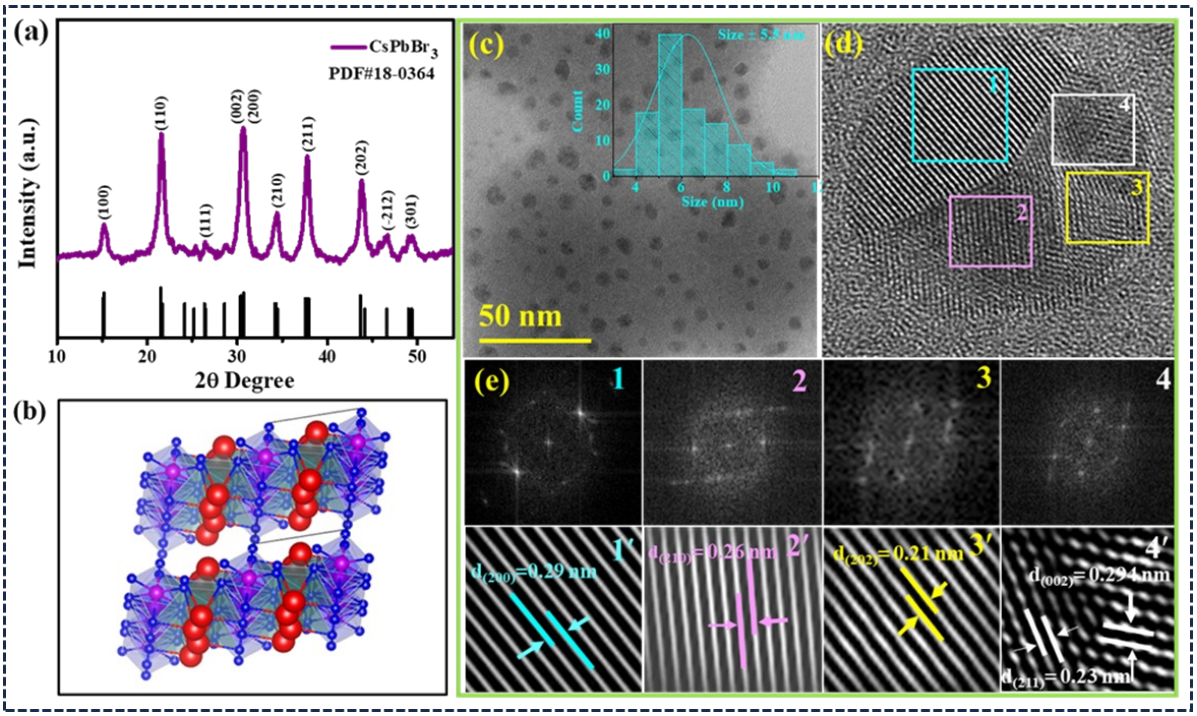

Figure S1. (a) The PXRD pattern of monoclinic $CsPbBr_3$ QDs. (b) Crystal structure of monoclinic $CsPbBr_3$ QDs. (c) TEM image of $CsPbBr_3$ QDs, and inset showing the corresponding size distribution. (d) High-resolution TEM image showing the different planes of the monoclinic $CsPbBr_3$ QDs (e) fast Fourier transformed (FFT) (1–4) and inverse FFT (1′–4′) images corresponding to the selected area shown in figure (d).

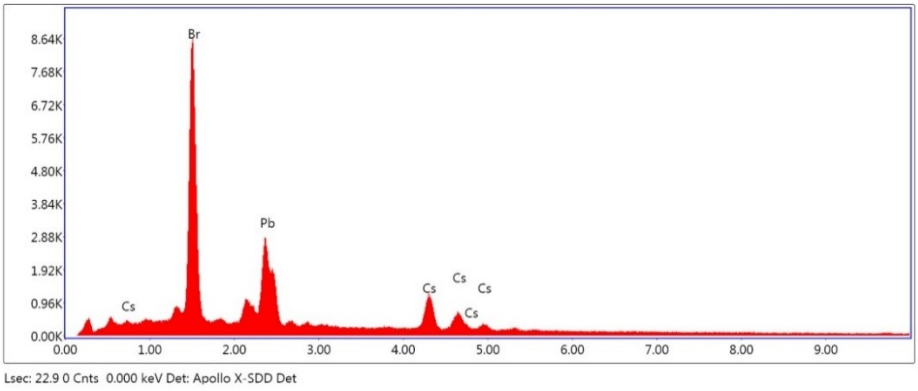

Figure S2. EDX spectrum of $CsPbBr_3$ QDs showing the presence of elements Cs, Pb, and Br.

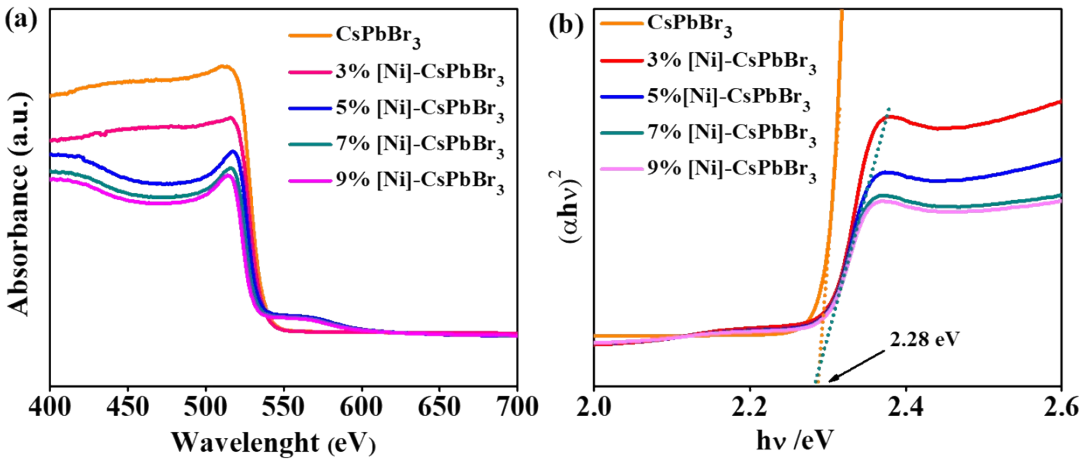

Figure S3. (a) The UV-visible diffuse reflectance spectra (UV-DRS) of $CsPbBr_3$ QDs exhibiting absorption maximum at 515 nm whereas its derivative photocatalysts (3% [Ni]-$CsPbBr_3$, 5% [Ni]-$CsPbBr_3$, 7% [Ni]-$CsPbBr_3$, and 9% [Ni]-$CsPbBr_3$) exhibiting absorption maxima at 517 nm, showing no significant change in absorption peaks after cocatalyst loading. Notably, $Ni(dmgH)_2$ complex showed a broad absorption peak at 563 nm for metal-to-ligand charge transfer (MLCT). (b) Tauc plots of $CsPbBr_3$ QDs and cocatalyst-loaded [Ni]-$CsPbBr_3$ photocatalyst systems.

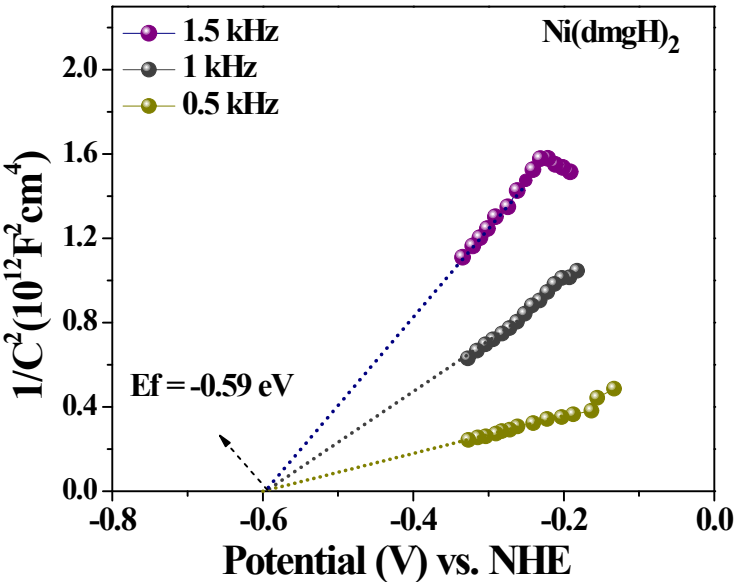

Figure S4. Mott-Schottky plot of confirmed the LUMO energy barrier of $Ni(dmgH)_2$ enough lower than the conduction band of $CsPbBr_3$ photocatalyst for activation of molecular oxygen molecules.

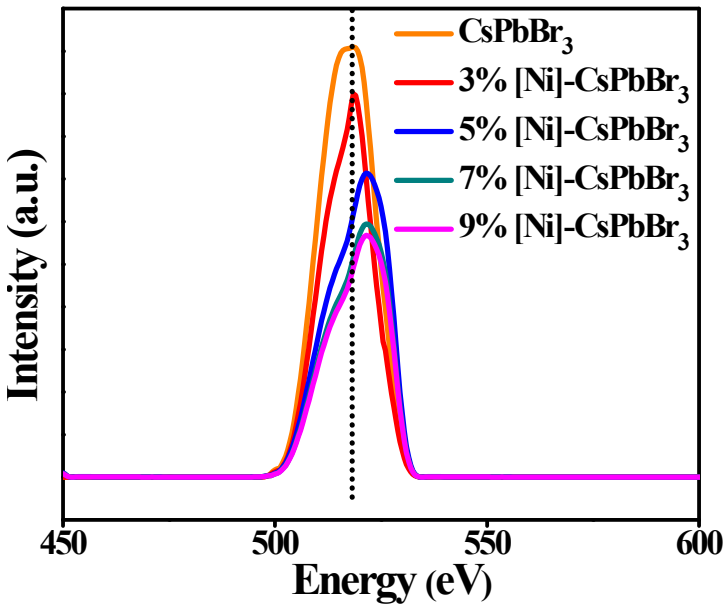

Figure S5. Photoluminescence spectra of the photocatalytic systems. The PL spectrum of pristine $CsPbBr_3$ QDs showed peak at 517 nm. The fluorescence intensity is gradually decreased with increasing loading of $Ni(dmgH)_2$. This trend suggests a reduction in the recombination process of photogenerated electron-hole pairs.

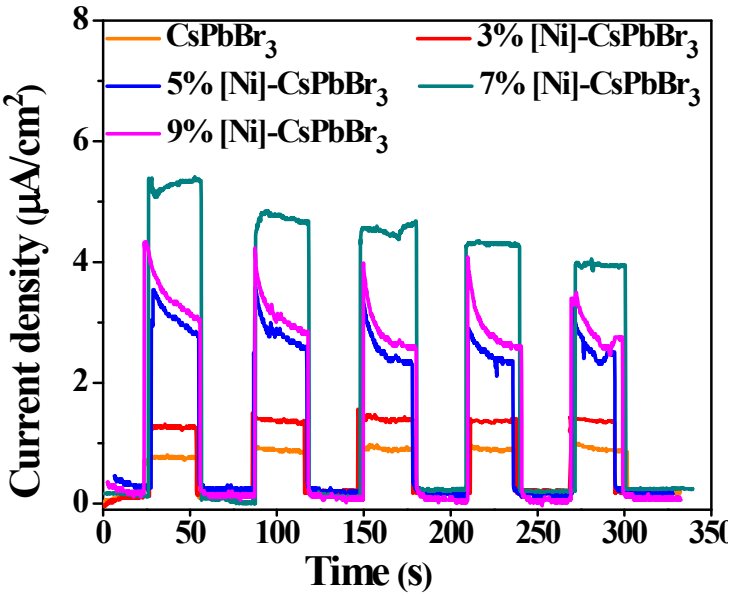

Figure S6. The photocurrent experiment confirmed the charge transfer and separation of all photocatalysts. As expected, the introduction of $N(dmgH)_2$ into $CsPbBr_3$ demonstrated significantly improved photocurrents compared to $CsPbBr_3$ and 7% [Ni]-$CsPbBr_3$ showing the highest photocurrent response as compared to other compositions. Photocurrent measurements were carried out in 0.1 M $TBAPF_6$ in ethyl acetate (electrolyte) and catalyst-coated FTO (working electrode), Ag/AgCl (reference electrode), and Pt wire used as a counter electrode. 15 W LED.

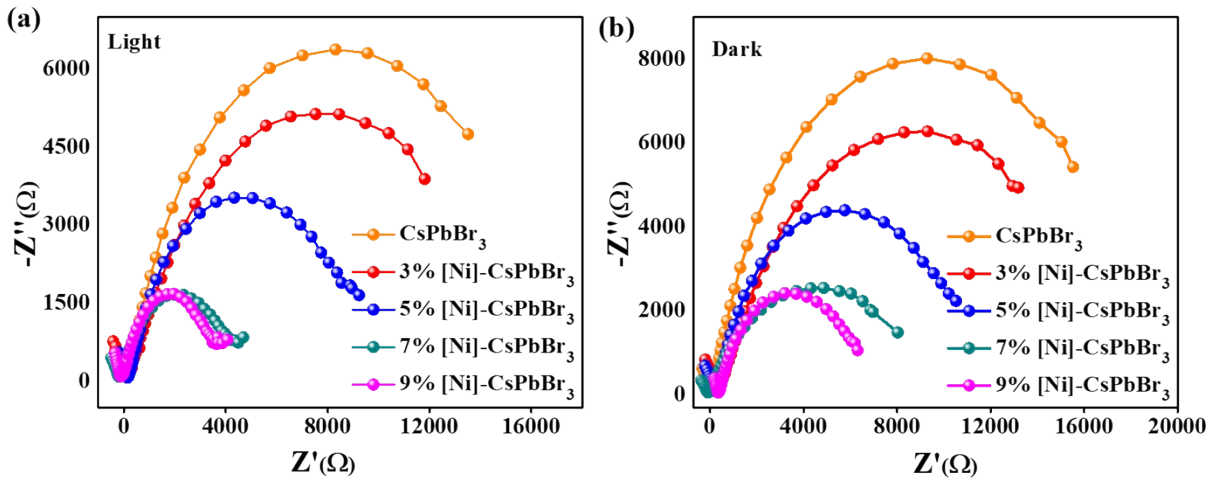

Figure S7. (a) Electrochemical impedance spectra were performed in light and dark conditions. The semi-arcs in the lower frequency range of the Nyquist plots gradually decrease with increasing amounts of $Ni(dmgH)_2$. Upon fitting with a simple R_{ct} equivalent circuit model, the resulting charge transfer resistance was reduced after the introduction of $Ni(dmgH)_2$ with $CsPbBr_3$. 7% [Ni]-$CsPbBr_3$ shows the smallest semi-arcs and low charge resistance.

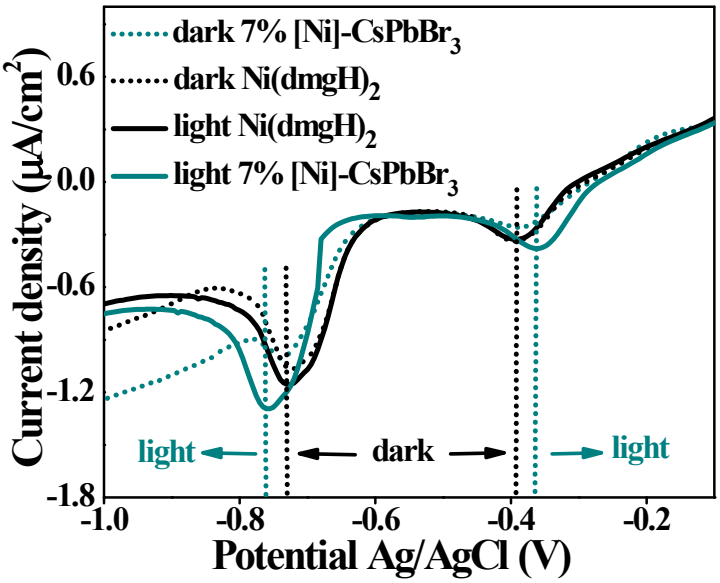

Figure S8. Differential pulse voltammograms (DPV) of $CsPbBr_3$ and 7% [Ni]-$CsPbBr_3$ in dark and light. The DPV was performed in 0.1 M $TBHPF_6$ ethyl acetate solution at a scan rate of 5 mV s^{-1}. DPV plot confirmed that the LUMO slightly shifted to more negative reduction potential and HOMO shifted to positive oxidation potential in the presence of light.

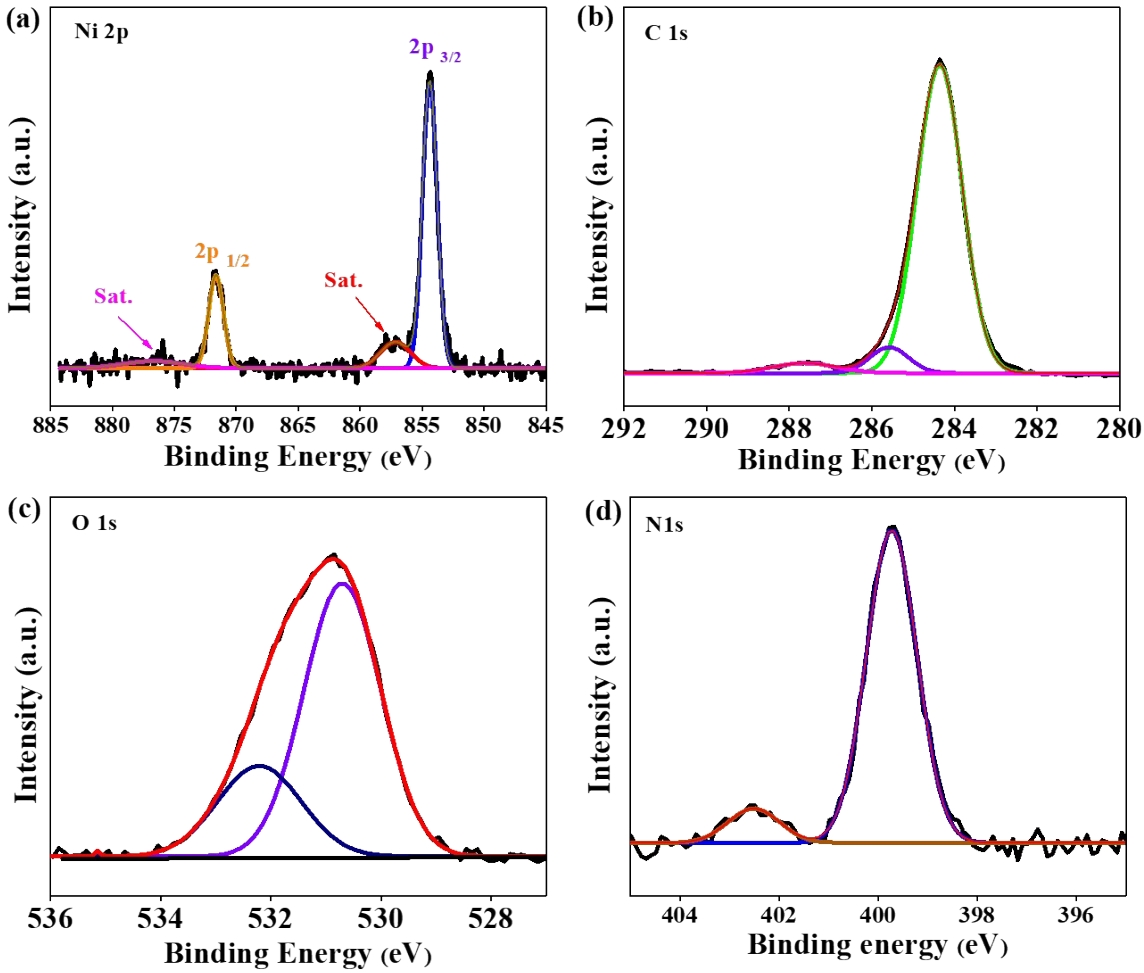

Figure S9. (a) Ni 2p XPS of 7% [Ni]-$CsPbBr_3$ showing the presence of Ni^{2+} species. (b) C 1s XPS of 7% [Ni]-$CsPbBr_3$ showing C=O and C=C bonds at 287.64 eV and 285.59 eV, respectively, while the peak at 284.37 eV is associated with carbon. (c) O 1s XPS of 7% [Ni]-$CsPbBr_3$ showing the presence of oxygen of adsorbed water (530.71 eV) and –OH group of the ligand of $Ni(dmgh)_2$ (532.23 eV). (d) N 1s XPS of 7% [Ni]-$CsPbBr_3$ showing the peak for C=N bond (399.7 eV) and N-O species (402.34 eV).[2]

Table S2. Optimization of photoredox C–N coupling reaction conditions

S.N.	Photocatalyst	Cocatalyst (Wt.%)	Solvent	Light	Time (h)	Yield (%)
Variation of cocatalysts						
1	$CsPbBr_3$	7 wt.% Ni-salen	Tetrahydrofuran	Blue LED	18	75
2	$CsPbBr_3$	7 wt.% $Ni(acac)_2$	Tetrahydrofuran	Blue LED	18	70
3	**$CsPbBr_3$**	**7 wt.% $Ni(dmgH)_2$**	**Tetrahydrofuran**	**Blue LED**	**18**	**92**
4	$CsPbBr_3$	7 wt.% $Ni(OAc)_2.4H_2O$	Tetrahydrofuran	Blue LED	18	49
Variation of wt.% $Ni(dmgH)_2$						
5	$CsPbBr_3$	3 wt.% $Ni(dmgH)_2$	Tetrahydrofuran	Blue LED	18	63
6	$CsPbBr_3$	5 wt.% $Ni(dmgH)_2$	Tetrahydrofuran	Blue LED	18	84
7	$CsPbBr_3$	7 wt.% $Ni(dmgH)_2$	Tetrahydrofuran	Blue LED	18	92
8	$CsPbBr_3$	9 wt.% $Ni(dmgH)_2$	Tetrahydrofuran	Blue LED	18	81
Variation of solvents						
9	$CsPbBr_3$	7 wt.% $Ni(dmgH)_2$	Acetonitrile	Blue LED	18	64
10	$CsPbBr_3$	7 wt.% $Ni(dmgH)_2$	Tetrahydrofuran	Blue LED	18	92
11	$CsPbBr_3$	7 wt.% $Ni(dmgH)_2$	1,4-Dioxane	Blue LED	18	81
12	$CsPbBr_3$	7 wt.% $Ni(dmgH)_2$	Toluene	Blue LED	18	58
Other variations in the reaction conditions						
13	-	-	Tetrahydrofuran	Blue LED	18	No Reaction
14	-	7 wt.% $Ni(dmgH)_2$	Tetrahydrofuran	Blue LED	18	No Reaction
15	$CsPbBr_3$	-	Tetrahydrofuran	Blue LED	18	48
16	$CsPbBr_3$	7 wt.% $Ni(dmgH)_2$	Tetrahydrofuran	Dark	18	5%

Reaction conditions: 10 mg $CsPbBr_3$, 4-nitrobenzaldehyde (0.5 mmol), piperidine (1.0 mmol), solvent (3.0 mL), time 18 h, Air, and 15 W blue LED at 35±3 °C. The photocatalyst was separated from the reaction mixture by centrifugation at 15,000 rpm for 10 minutes. The product was separated by column chromatography in a silica column using different ratios of ethyl acetate and hexane as the eluent. ^1H and ^{13}C NMR spectra were used to detect the formation and purity of the product. Isolated yield was reported.

Table S3: The photocatalytic reaction of aliphatic aldehyde and benzyl amine.

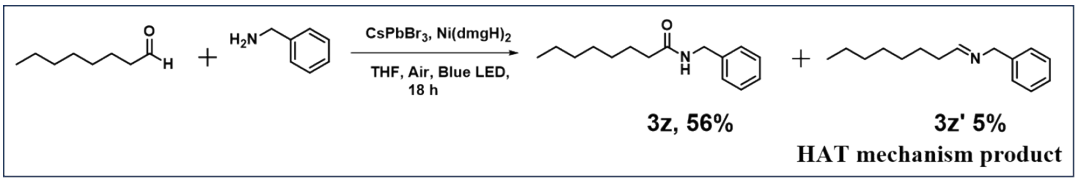

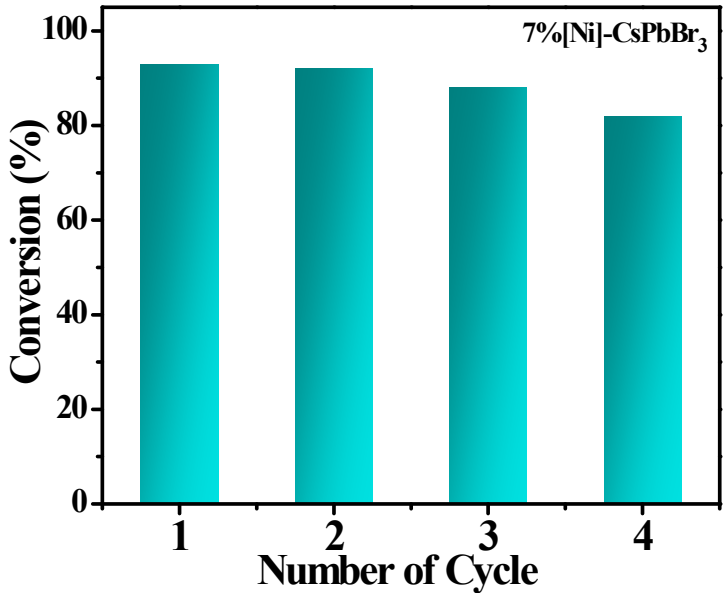

Figure S10. Photocatalytic recyclability test for amide bond formation.

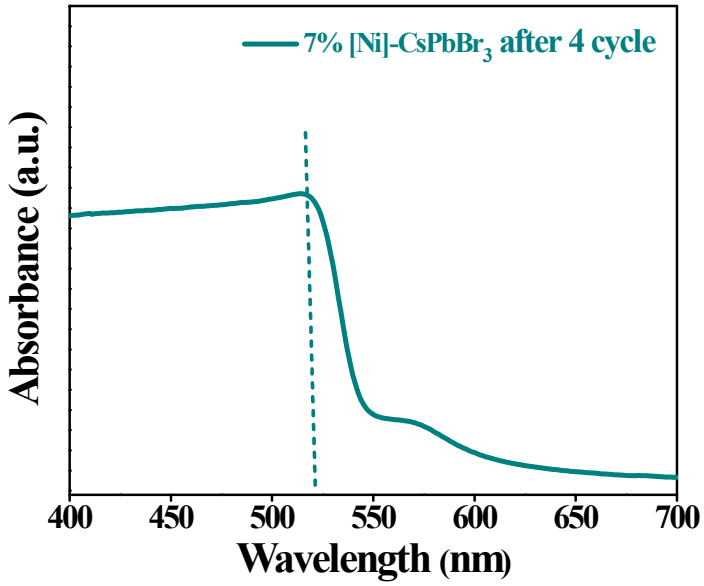

Figure S11. UV-vis spectra confirmed the absorption peak was not changed after 4 times recycling of 7%[Ni]-CsPbBr

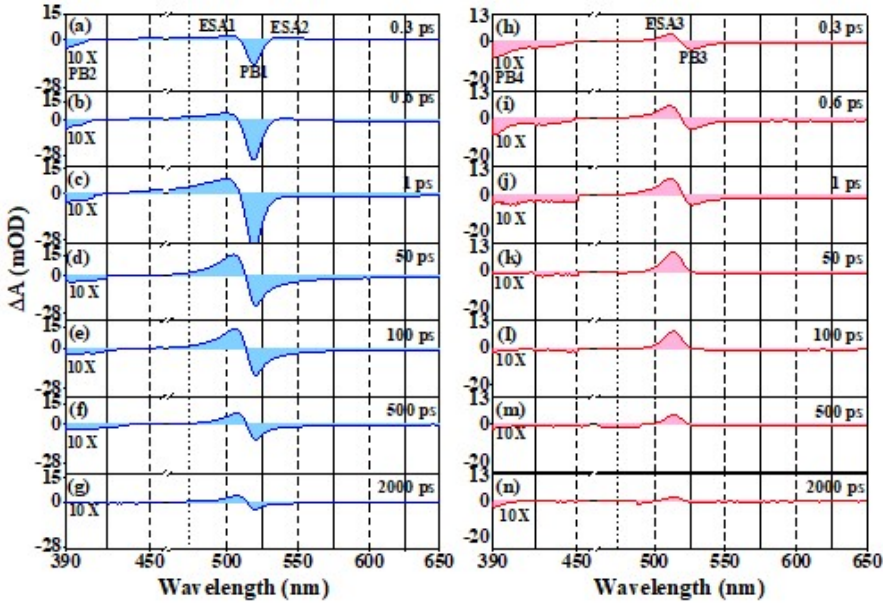

Figure S12. The transient absorption (TA) spectra at different delay times between pump and probe for $CsPbBr_3$ (a-g) and 7% [Ni]- $CsPbBr_3$ (h-n). The data from ~ 390 nm to 450 nm is magnified by ten times for better visualization. The delay times are mentioned along with the respective spectrum (PB = photo bleach; ESA = excited state absorption).

$$k_{et} = \frac{1}{\tau_{Ni-CsPbBr_3}} - \frac{1}{\tau_{CsPbBr_3}} \qquad \ldots.1$$

where $\tau_{Ni-CsPbBr_3}$represent the lifetime of the bleach recovery of the 7% [Ni]-$CsPbBr_3$ and τ_{CsPbBr_3} represent the lifetime of the bleach recovery of pristine $CsPbBr_3$ QDs.

Table S4. Fitting coefficient of kinetics traces at 400 nm, 500 nm, 550 nm, and 650 nm of $CsPbBr_3$ 7% [Ni]- $CsPbBr_3$ excited at 370 nm.

Catalyst	Wavelength (nm)	τ_1 (ps)	τ_2 (ps)	τ_3 (ps)
$CsPbBr_3$	400	40 ± 6	-	Long Lived
	500	98 ± 5 59 %	1368 ± 233 41 %	Long Lived
	550	60 ± 8 61 %	817 ± 165 39 %	Long Lived
	650	32 ± 3 75 %	434 ± 76 25 %	Long Lived
7% [Ni]-$CsPbBr_3$	400	20 ± 9	-	Long Lived
	500	41 ± 2 58 %	506 ± 50 41 %	Long Lived
	550	31 ± 3 54 %	293 ± 32 46 %	Long Lived
	650	22 ± 4 56 %	354 ± 63 44 %	Long Lived

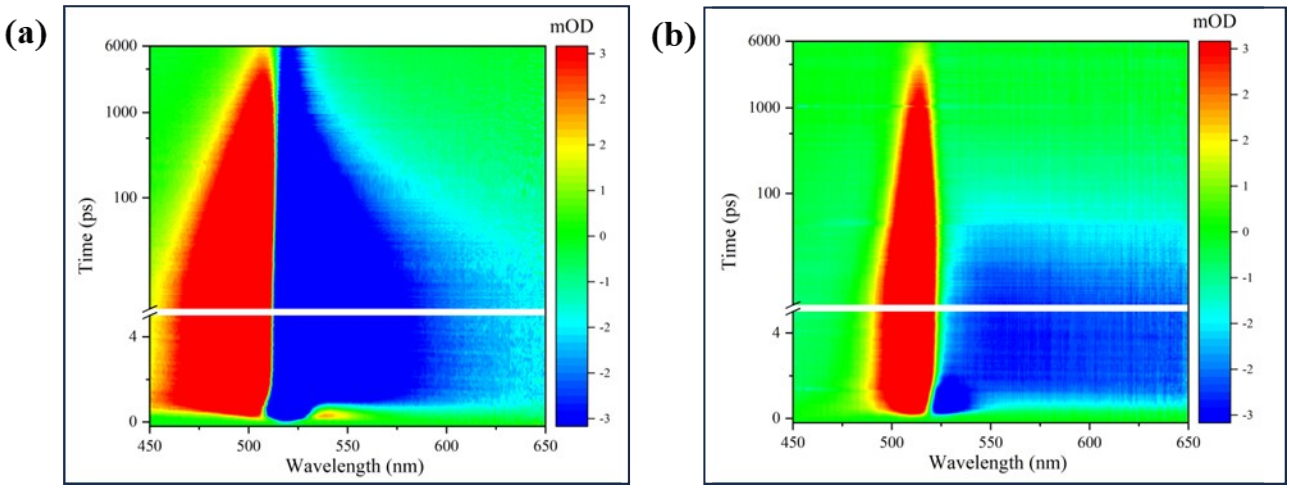

Figure S13. (a) TA spectra of $CsPbBr_3$, (b) TA spectra of 7% [Ni]-$CsPbBr_3$.

Quenching Experiments:

(a) Hole scavenger

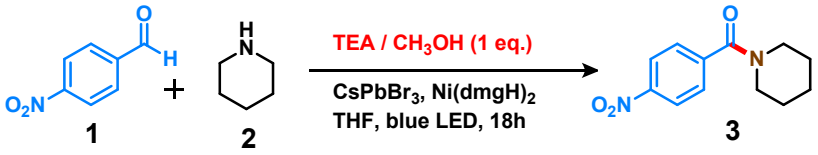

(b) Electron scavenger

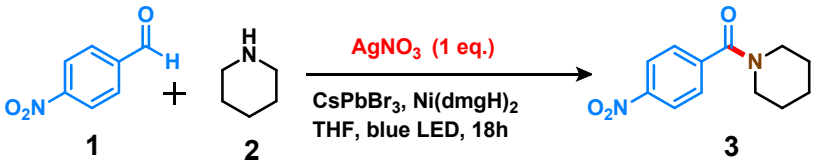

(c) Superoxide radical scavenger

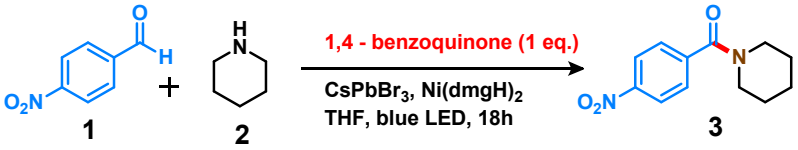

(d) Free radical scavenger

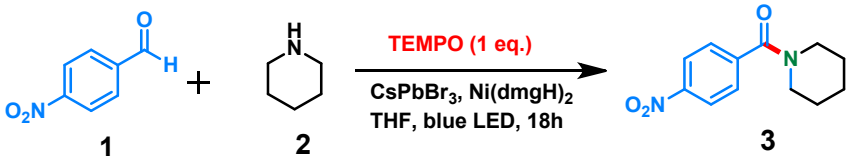

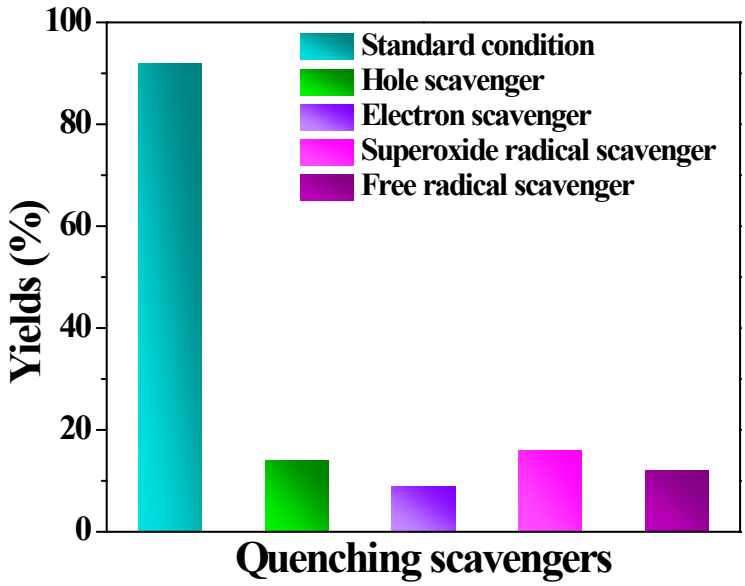

Figure S14. Quenching experiments with different types of scavengers.

(a)

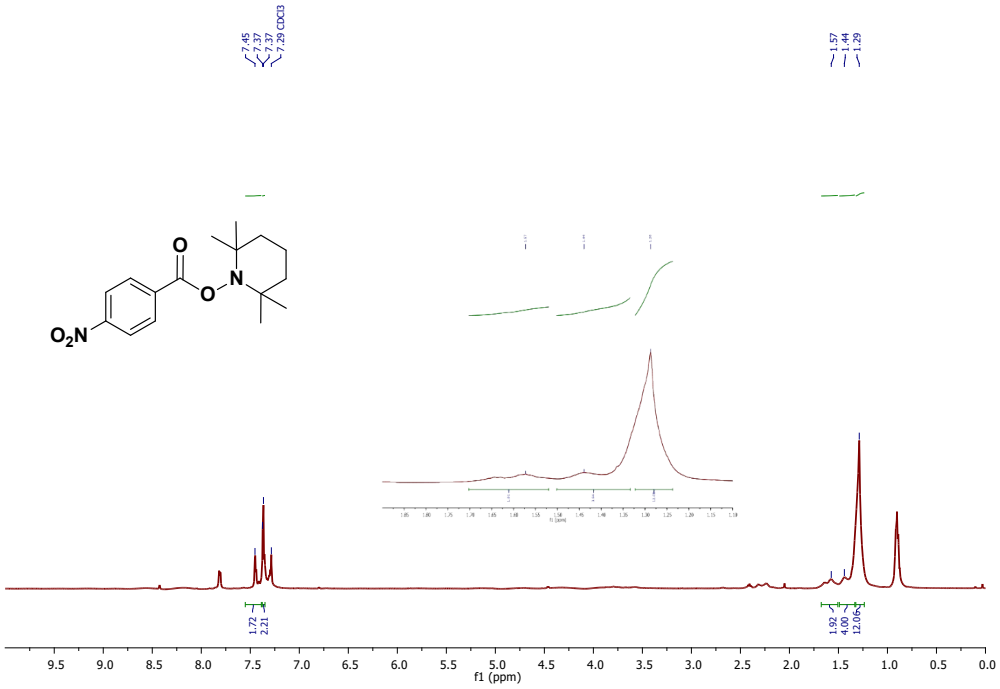

(b)

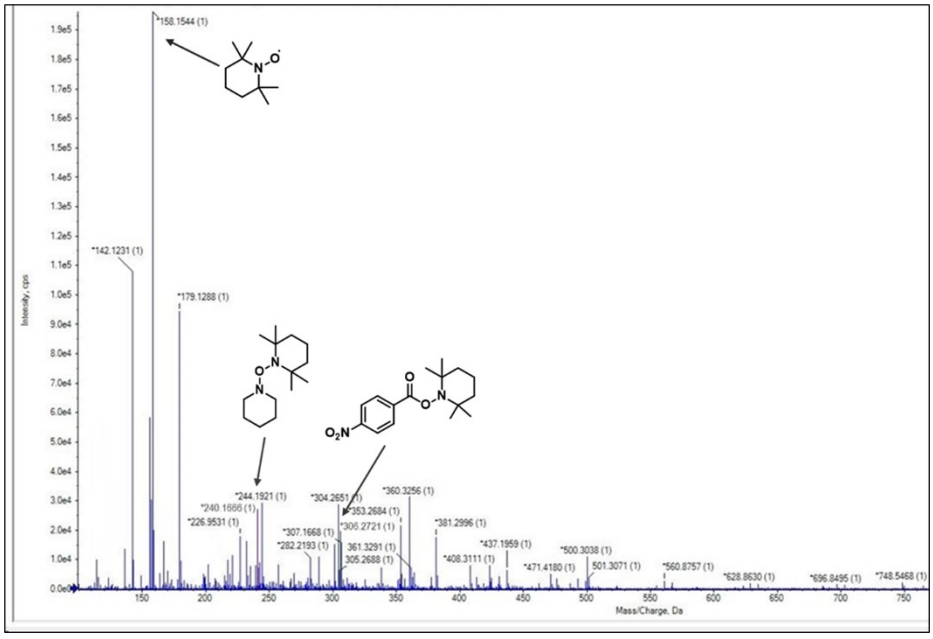

Figure S15. (a) ^{1}H NMR and (b) mass spectrometry data of the reaction intermediate radicals trapped by 2,2,6,6-tetramethyl-1-piperidinyloxy (TEMPO).

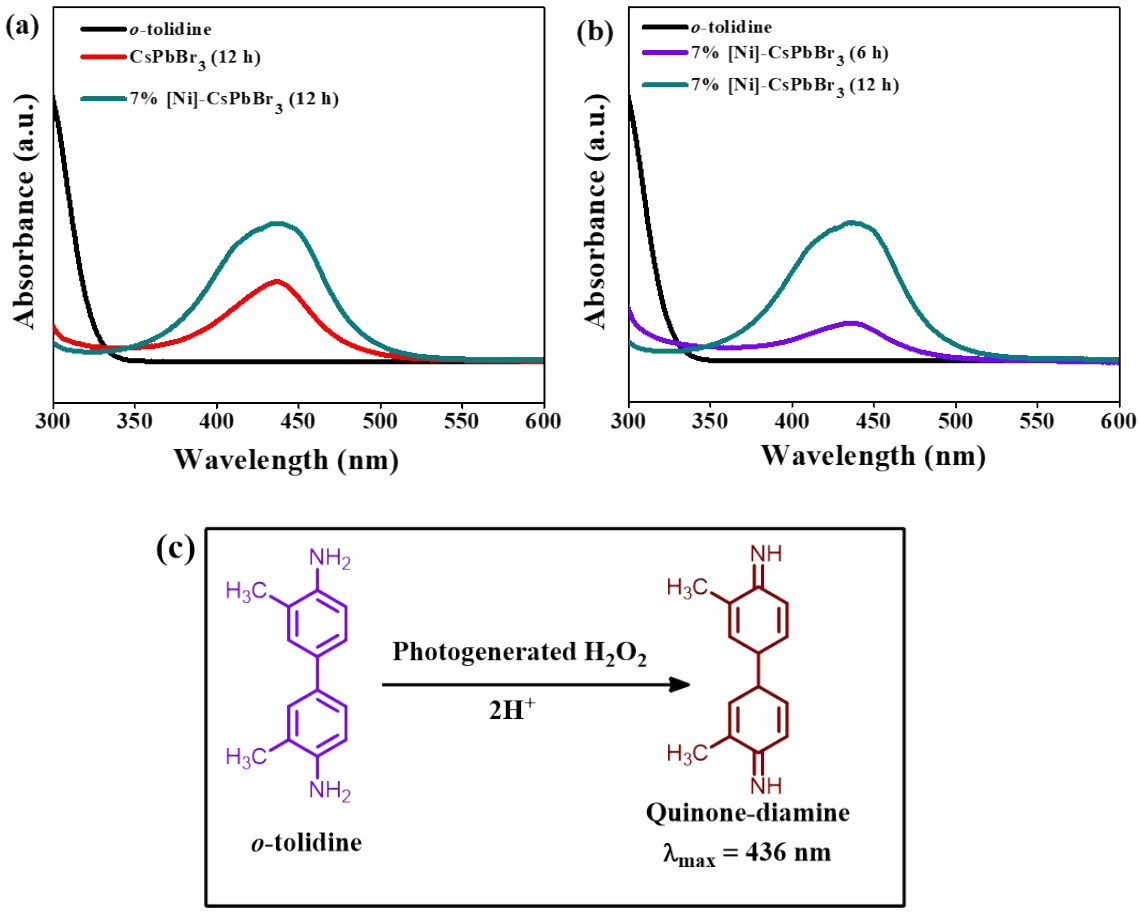

Figure S16. (a) Detection of H_2O_2, formed by the photoredox reaction with $CsPbBr_3$ and 7% [Ni]-$CsPbBr_3$. (b) Detection of H_2O_2, formed by the photoredox reaction with 7% [Ni]-$CsPbBr_3$ at different times.

Reaction conditions

After the photoredox reaction, the catalyst was separated via centrifugation. Further, photoredox reaction-generated H_2O_2 from the reaction mixture was extracted into 2 mL of water. Subsequently, 10 µL *o*-tolidine solution (1 wt. % of tolidine in 0.1 M HCl) was added to the H_2O_2-containing solution, and UV-visible spectra were recorded. The oxidation of *o*-tolidine by photogenerated H_2O_2 resulted a yellow-colored compound (with a maximum absorption at 436 nm).[3,6]

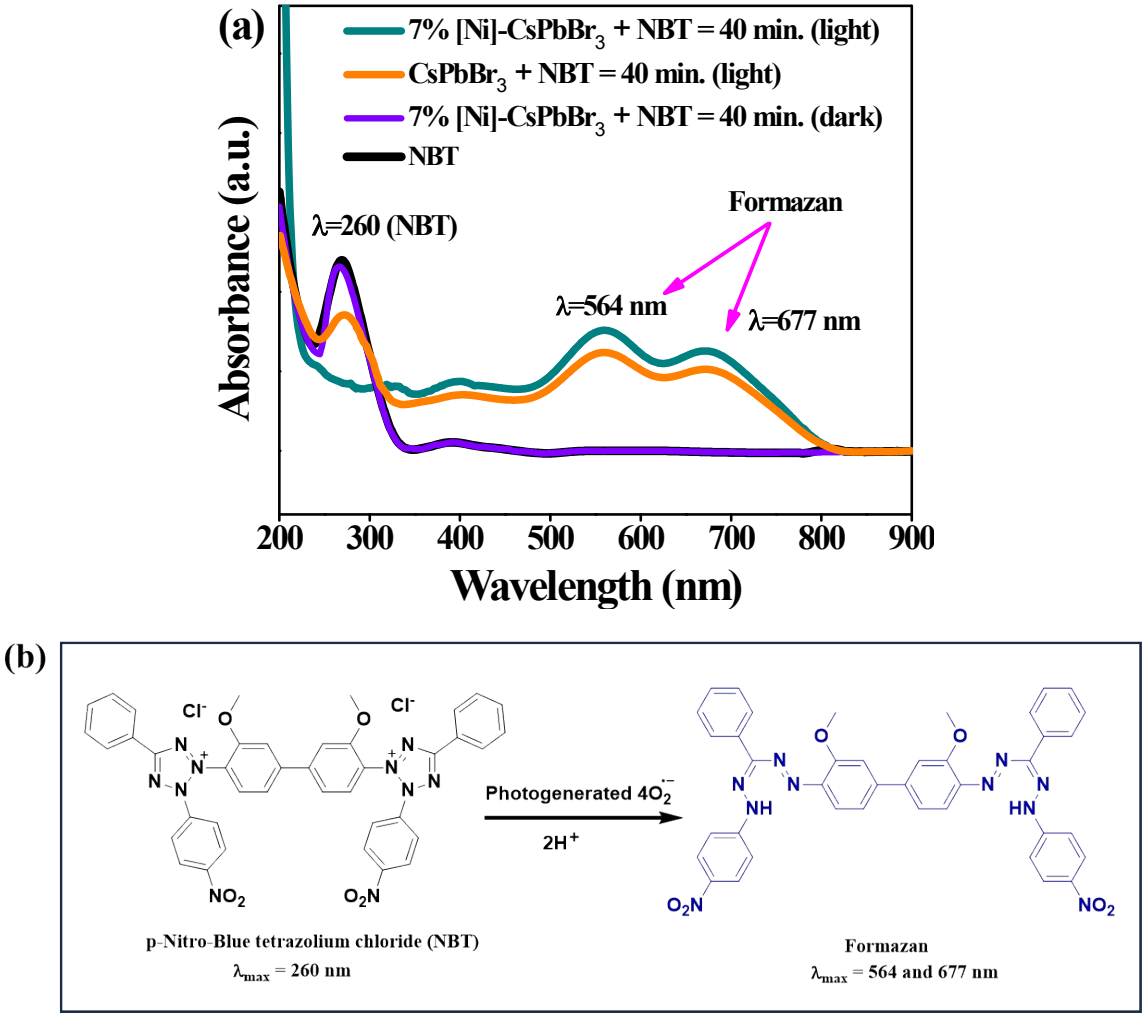

Figure S17. Detection of superoxide radicals formed by the reduction of dioxygen during photocatalytic process.

Reaction conditions: The detection of photogenerated $O_2^{\bullet-}$ by 7% [Ni]-$CsPbBr_3$ was performed using p-Nitro-blue tetrazolium chloride (NBT) as the indicator. In the presence of $O_2^{\bullet-}$, NBT undergoes reduction to form blue formazan with λ_{max} values of 564 and 677 nm. As depicted in Figure S17, two absorption peaks were observed for 7% [Ni]-$CsPbBr_3$ + NBT after 40 minutes of light exposure. These results conclusively demonstrate the ability of 7% [Ni]-$CsPbBr_3$ to generate $O_2^{\bullet-}$ at light, thereby confirming its role in driving the photocatalytic amide C–N coupling reaction.

Table S5: Characterization of the products by ^{1}H NMR and ^{13}C NMR spectroscopy[7-10]

3a: phenyl(piperidin-1-yl) methanone 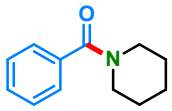	^{1}H NMR (500 MHz, $CDCl_3$) δ: 7.40 (m, 5H), 3.73 (dd, 2H), 3.35 (dd, 2H), 1.68 (m, 4H), 1.49 (m, 2H). ^{13}C NMR (125 MHz, $CDCl_3$) δ: 170.44, 136.41, 129.38, 128.39, 126.81, 48.77, 43.18, 26.04, 25.24, 24.58. Yield: 78%, 74 mg and 0.39 mmol
3b: (4-methylphenyl)(piperidin-1-yl) methanone[7] 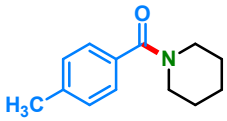	^{1}H NMR (500 MHz, $CDCl_3$) δ: 7.31 (d, J = 8.0 Hz, 2H), 7.20 (d, J = 7.8 Hz, 2H), 3.71 (m, 2H), 3.37 (m, 2H), 2.38 (s, 3H), 1.61 (m, 6H). ^{13}C NMR (125 MHz, $CDCl_3$) δ: 170.58, 139.44, 133.50, 128.98, 126.93, 48.93, 43.25, 29.69, 24.63, 21.35. Yield: 77%, 78 mg and 0.38 mmol
3c: (4-methoxyphenyl)(piperidin-1-yl)methanone[7] 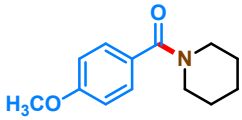	^{1}H NMR (500 MHz, $CDCl_3$) δ: 7.38 (d, J = 8.7 Hz, 2H), 6.91 (d, J = 8.7 Hz, 2H), 3.83 (s, 3H), 3.57 (m, 4H), 1.64 (m, 6H). ^{13}C NMR (125 MHz, $CDCl_3$) δ: 170.30, 160.52, 128.85, 128.64, 113.63, 54.02, 24.66. Yield**:** 74%, 81 mg and 0.36 mmol
3d: Dimethoxyphenyl(piperidin-1-yl) methanone 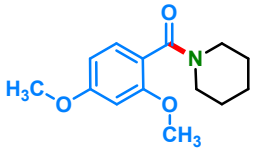	^{1}H NMR (500 MHz) δ: 6.95 (d, J = 9.6 Hz, 2H), 6.85 (s, 1H), 3.88 (s, 6H), 3.58 (dd, 4H), 1.62 (d, 6H). ^{13}C NMR (125 MHz, $CDCl_3$) δ: 170.25, 150.02, 148.86, 128.74, 119.79, 110.70, 110.49, 56.01, 26.28, 25.72, 24.63. Yield: 72%, 90 mg and 0.36 mmol
3e: (4-bromophenyl)(piperidin-1-yl) methanone 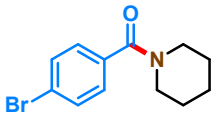	^{1}H NMR (500 MHz, $CDCl_3$) δ: 7.57 (d, *J* = 8.4 Hz, 1H), 7.31 (d, *J* = 8.4 Hz, 1H), 3.73 (dd, 2H), 3.36 (dd, 2H), 1.63 (d, 6H). ^{13}C NMR (125 MHz, $CDCl_3$) δ: 169.31, 135.26, 131.64, 128.59, 123.66, 48.84, 43.30, 26.10, 25.54, 24.52. Yield: 89%, 103 mg and 0.44 mmol
3f: (2-nitrophenyl)(piperidin-1-yl) methanone 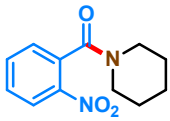	^{1}H NMR (500 MHz, $CDCl_3$) δ: 8.19 (d, J = 8.3 Hz, 1H), 7.70 (t, J = 7.5 Hz, 1H), 7.56 (t, J = 7.9 Hz, 1H), 7.39 (d, J = 7.6 Hz, 1H), 3.77 (m, 2H), 3.17 (m, 2H), 1.79–1.46 (m, 6H). ^{13}C NMR (125 MHz, $CDCl_3$) δ: 166.25, 145.25, 134.41, 133.46, 129.57, 128.00, 124.73, 47.95, 42.73, 25.81, 25.13, 24.46. Yield: 87%, 101 mg and 0.43 mmol

3g: (3-nitrophenyl)(piperidin-1-yl) methanone[8] 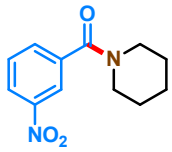	^{1}H NMR (500 MHz, $CDCl_3$) δ: 8.26 (d, J = 7.6 Hz, 2H), 7.74 (d, J = 7.3 Hz, 1H), 7.61 (t, J = 7.8 Hz, 1H), 3.73 (s, 2H), 3.34 (s, 2H), 1.63 (d, J = 77.4 Hz, 6H). ^{13}C NMR (125 MHz, $CDCl_3$) δ: 167.61, 148.05, 138.05, 132.90, 129.74, 124.23, 122.05, 48.84, 43.37, 26.52, 25.49, 24.40. Yield: 82%, 96 mg and 0.41 mmol
3h: (4-nitrophenyl)(piperidin-1-yl) methanone[7] 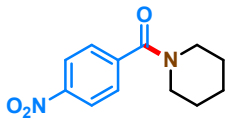	^{1}H NMR (500 MHz, $CDCl_3$) δ 8.28 (d, J = 8.7 Hz, 2H), 7.59 – 7.55 (d, 2H), 3.74 (m, 2H), 3.30 (m, 2H), 1.63 (m, 6H). ^{13}C NMR (125 MHz, CDCl3) δ 167.92, 148.22, 142.70, 127.81, 123.85, 48.66, 43.22, 26.52, 25.51, 24.40. Yield: 92%, 107.5 mg, and 0.46 mmol
3i: Piperidin-1yl(3-(trifluoromethyl) phenyl)methanone[8] 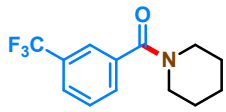	^{1}H NMR (500 MHz, $CDCl_3$) δ: 7.67 (s, 1H), 7.61 – 7.52 (m, 3H), 3.73 (t, 2H), 3.34 (m, 2H), 1.71 (m, 4H), 1.55 (m, 2H). ^{13}C NMR (125 MHz, $CDCl_3$) δ: 168.74, 137.24, 130.14, 129.04, 126.18, 124.82, 123.87, 122.65, 48.80, 25.50, 24.47. Yield: 84%, 108 mg and 0.42 mmol
3j: Morpholino(phenyl)methanone[9] 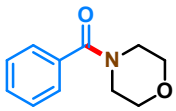	^{1}H NMR (500 MHz, $CDCl_3$) δ: 7.42 (s, 5H), 3.83–3.42 (m, 8H). ^{13}C NMR (125 MHz, $CDCl_3$) δ: 170.50, 135.28, 129.92, 128.58, 127.09, 66.90, 48.19. Yield: 76%, 72 mg and 0.37 mmol
3k:(4-Chlorophenyl)(morpholino)methanone 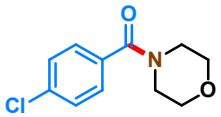	^{1}H NMR (500 MHz, $CDCl_3$) δ: 7.73 – 7.68 (m, 2H), 7.23 (d, *J* = 11.2 Hz, 2H), 4.22 – 4.10 (d, 4H), 4.01 (d, 4H). ^{13}C NMR (125 MHz, $CDCl_3$) δ: 171.46 (s), 161.93 (s), 130.21 (s), 128.32 (s), 114.81 (s), 67.92 (s), 56.36 (s). Yield: 83%, 93 mg and 0.41 mmol
3l: (4-bromophenyl)(morpholino) methanone[8] 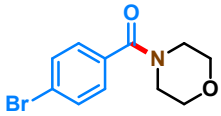	^{1}H NMR (500 MHz, $CDCl_3$) δ: 7.40 (d, J = 8.7 Hz, 2H), 6.92 (d, J = 8.7 Hz, 2H), 3.84 (d, 2H), 3.70 (d, 2H), ^{13}C NMR (125 MHz, $CDCl_3$) δ: 170.44, 160.93, 129.20, 127.33, 113.80, 66.92, 55.36. Yield: 81%, 108 mg and 0.40 mmol
3m: phenyl(pyrrolidine-1-yl) Methanone[7]	^{1}H NMR (600 MHz, CDCl3) δ: 7.49 (d, J = 6.4 Hz, 2H), 7.37

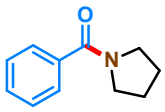	(d, J = 5.5 Hz, 3H), 3.63 (t, 2H), 3.40 (t, 2H), 1.89 (dt, 4H). ^{13}C NMR (150 MHz, $CDCl_3$) δ: 169.80, 137.10, 129.80, 128.23, 127.05, 49.62, 46.19, 26.35, 24.43. Yield: 76%, 66 mg and 0.37 mmol
3n: (4-methylphenyl)(pyrrolidin-1-yl) methanone[8] 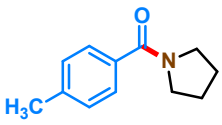	^{1}H NMR (600 MHz, $CDCl_3$) δ: 7.34 (d, *J* = 7.4 Hz, 2H), 7.11 (d, *J* = 7.4 Hz, 2H), 3.56 (t, 2H), 3.36 (t, 2H), 2.29 (s, 3H), 1.83 (m, 4H). ^{13}C NMR (150 MHz, $CDCl_3$) δ: 169.90, 139.94, 134.22, 128.82, 127.20, 49.68, 46.22, 26.40, 24.45, 21.38. Yield: 74%, 70 mg and 0.36 mmol
3o: (4-chlorophenyl)(piperidin-1-yl) methanone[8] 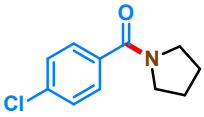	1H NMR (600 MHz, CDCl3) δ: 7.46 (d, J = 8.1 Hz, 2H), 7.37 (d, J = 8.2 Hz, 2H), 3.63 (t, 2H), 3.41 (t, 2H), 1.92 (dt, 4H). ^{13}C NMR (150 MHz, $CDCl_3$) δ: 168.64, 135.86, 135.44, 128.66, 128.52, 49.64, 46.33, 26.40, 24.40. Yield: 83%, 86.5 mg and 0.41 mmol
3p: (4-nitrophenyl)(piperidin-1-yl) methanone[7] 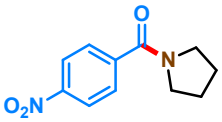	^{1}H NMR (600 MHz, CDCl3) δ: 8.25 (d, J = 8.0 Hz, 2H), 7.67 (d, J = 7.9 Hz, 2H), 3.65 (t, 2H), 3.37 (t, 2H), 1.95 (dt, 2H), 1.84 – 1.78 (m, 2H). ^{13}C NMR (150 MHz, $CDCl_3$) δ: 167.43, 148.40, 143.08, 128.14, 123.68, 49.45, 46.39, 26.35, 24.34. Yield: 89%, 97 mg and 0.44 mmol
3q: (2-hydroxyphenyl)(pyrrolidin-1-yl)methanone 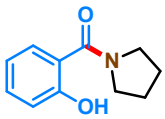	^{1}H NMR (500 MHz, $CDCl_3$) δ: 7.19 (t, *J* = 7.9 Hz, 1H), 7.11 (s, 1H), 6.95 (d, *J* = 7.6 Hz, 1H), 6.90 (dd, *J* = 8.2, 2.5 Hz, 1H), 3.64 (t, 2H), 3.42 (t, 2H), 1.91 (dt, 4H). ^{13}C NMR (126 MHz, $CDCl_3$) δ: 170.19, 157.07, 137.39, 129.31, 117.79, 117.52, 114.49, 49.68, 46.30, 26.15, 24.29. Yield: 56%, 54 mg and 0.41 mmol
3r: Phenylenebis(pyrrolidine-1-yl) methanone 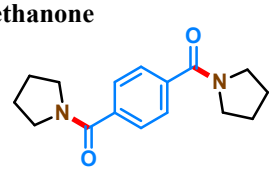	^{1}H NMR (500 MHz, $CDCl_3$) δ: 7.56 (s, 1H), 3.67 (t, 2H), 3.42 (t, 2H), 2.01 – 1.97 (m, 2H), 1.91 (d, 2H). ^{13}C NMR (125 MHz, $CDCl_3$) δ: 169.05, 138.54, 127.06, 49.54, 46.22, 26.37, 24.44. Yield: 69%, 93 mg and 0.34 mmol
3s: pyrrolodin-1-yl(thiophene-2-yl)methanone[10]	^{1}H NMR (500 MHz, $CDCl_3$) δ: 7.54 (d, *J* = 3.7 Hz, 1H), 7.48 (d, *J* = 5.0 Hz, 1H), 7.09 (m, 1H), 3.73 (m, 4H), 1.99 (m, 4H).

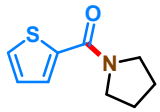	^{13}C NMR (125 MHz, $CDCl_3$) δ: 161.89, 139.48, 129.62, 129.57, 127.05, 48.93, 47.34, 26.72, 24.08. Yield: 83%, 75 mg and 0.41 mmol
3t: Pyridin-2yl(pyrrolidin-1-yl) methanone[10] 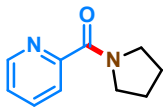	^{1}H NMR (500 MHz, $CDCl_3$) δ: 8.50 (d, 1H), 7.72 (m, 2H), 7.26 (d, 1H), 3.62 (m, 4H), 1.84 (m, 4H). ^{13}C NMR (126 MHz, $CDCl_3$) δ: 166.47, 154.42, 147.93, 136.79, 124.63, 123.70, 49.01, 46.77, 26.49, 23.96. Yield: 80%, 70 mg, and 0.40 mmol
3u: 3-benzoyloxzolidin-2-one 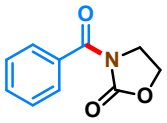	^{1}H NMR (500 MHz, $CDCl_3$) δ: 7.68 (dd, J = 8.2, 1.0 Hz, 2H), 7.57 (t, J = 7.5 Hz, 1H), 7.45 (t, J = 7.8 Hz, 2H), 4.49 (t, 2H), 4.18 (t, 2H). ^{13}C NMR (125 MHz, $CDCl_3$) δ: 169.82, 153.25, 132.66, 132.40, 129.09, 127.89, 62.27, 43.72. Yield: 71%, 67 mg and 0.35 mmol
3v: N-(pyridin-2-yl)benzamide 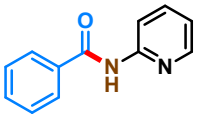	^{1}H NMR (500 MHz, $CDCl_3$) δ: 9.37 (s, 1H), 8.46 (d, J = 8.4 Hz, 1H), 8.23 – 8.13 (m, 1H), 7.99 (d, J = 7.2 Hz, 2H), 7.79 (s, 1H), 7.57 (d, J = 8.6 Hz, 1H), 7.52 (d, J = 7.8 Hz, 2H), 7.08 (s, 1H). ^{13}C NMR (125 MHz, $CDCl_3$) δ: 171.23, 166.08, 151.75, 147.50, 138.75, 134.26, 132.25, 129.97, 128.78, 127.48, 119.89, 114.57. Yield: 70%, 69 mg and 0.35 mmol
3w: N-(Quinolin-7-yl) benzamide 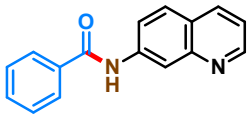	^{1}H NMR (500 MHz, $CDCl_3$) δ: 10.78 (s, 1H), 8.97 (d, J = 7.6 Hz, 1H), 8.87 (d, J = 5.8 Hz, 1H), 8.21 (dd, J = 8.2, 1.4 Hz, 1H), 8.12 (dd, J = 8.0, 1.5 Hz, 2H), 7.60 (m, 5H), 7.50 (dd, 1H). ^{13}C NMR (125 MHz, $CDCl_3$) δ: 165.49, 148.31, 138.82, 136.41, 135.21, 134.63, 131.85, 128.82, 128.03, 127.49, 127.32, 121.70, 116.58. Yield: 76%, 94 mg and 0.38 mmol
3x: N-(2-(pyridin-2-yl)ethyl)benzamide 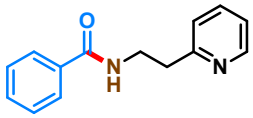	^{1}H NMR (500 MHz, $CDCl_3$) δ: 8.54 (d, J = 4.8 Hz, 1H), 7.78 (d, J = 7.1 Hz, 2H), 7.63 (t, J = 7.7 Hz, 2H), 7.48 – 7.38 (m, 3H), 7.22 – 7.15 (m, 2H), 3.88 – 3.83 (m, 2H), 3.10 (t, J = 6.3 Hz, 2H). ^{13}C NMR (125 MHz, $CDCl_3$) δ: 167.41, 159.74, 149.04, 136.92, 134.70, 131.27, 128.47, 123.64, 121.73, 39.30, 36.63. Yield: 67%, 76 mg and 0.34 mmol

3y: N-benzylbenzamide[11] 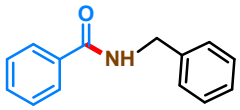	^{1}H NMR (500 MHz, $CDCl_3$) δ: 7.83 – 7.80 (d, 2H), 7.51 (d, J = 7.9 Hz, 1H), 7.44 (d, 2H), 7.37 (d, 4H), 7.33 (m, 1H), 6.55 (d, 1H), 4.67 (s, 2H). ^{13}C NMR (125 MHz, $CDCl_3$) δ: 167.35, 138.15, 134.43, 131.57, 128.80, 128.60, 127.93, 127.63, 126.99, 44.16 Yield: 72%, 75 mg and 0.35 mmol
3z: N-benzyloctanamide 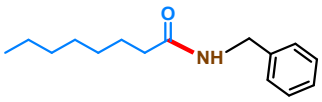	^{1}H NMR (500 MHz, $CDCl_3$) δ: 7.38 – 7.33 (d, 2H), 7.29 (t, J = 6.5 Hz, 3H), 6.00 – 5.86 (s, 1H), 4.47 (s, 2H), 3.05 (t, 2H), 2.26 – 2.20 (m, 2H), 1.72 – 1.65 (m, 2H), 1.35 – 1.28 (m, 6H), 0.91 (t, 3H). ^{13}CMR (125 MHz, $CDCl_3$) δ: 173.05, 128.69, 127.82, 127.47, 106.56, 43.58, 39.15, 36.77, 31.49, 29.69, 25.46, 22.39, 13.93. Yield: 55%, 64 mg and 0.27 mmol
3aa: N, N-diethyl benzamide 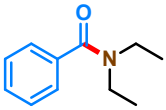	^{1}H NMR (500 MHz, CDCl3) δ: 7.42–7.36 (m, 5H), 3.42 (d, 4H), 1.20 (d, 6H). ^{13}C NMR (125 MHz, CDCl3) δ: 171.31, 137.32, 129.07, 128.38, 126.28, 43.29, 39.34, 14.15, 13.00. Yield: 62%, 54 mg and 0.30 mmol
3bb: N-propyl benzamide 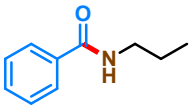	^{1}H NMR (600 MHz, $CDCl_3$) δ: 7.78 (d, *J* = 7.4 Hz, 2H), 7.49 (m, *J* = 7.1 Hz, 1H), 7.42 (t, *J* = 7.3 Hz, 2H), 6.39 (s, 1H), 3.42 (d, 2H), 1.64 (dd, 2H), 0.99 (t, 3H). ^{13}C NMR (150 MHz, $CDCl_3$) δ: 167.66, 134.87, 131.28, 128.51, 126.87, 41.77, 22.91, 11.44. Yield: 59%, 43.5 mg and 0.29 mmol

^{1}H and ^{13}C NMR spectra of **3a**

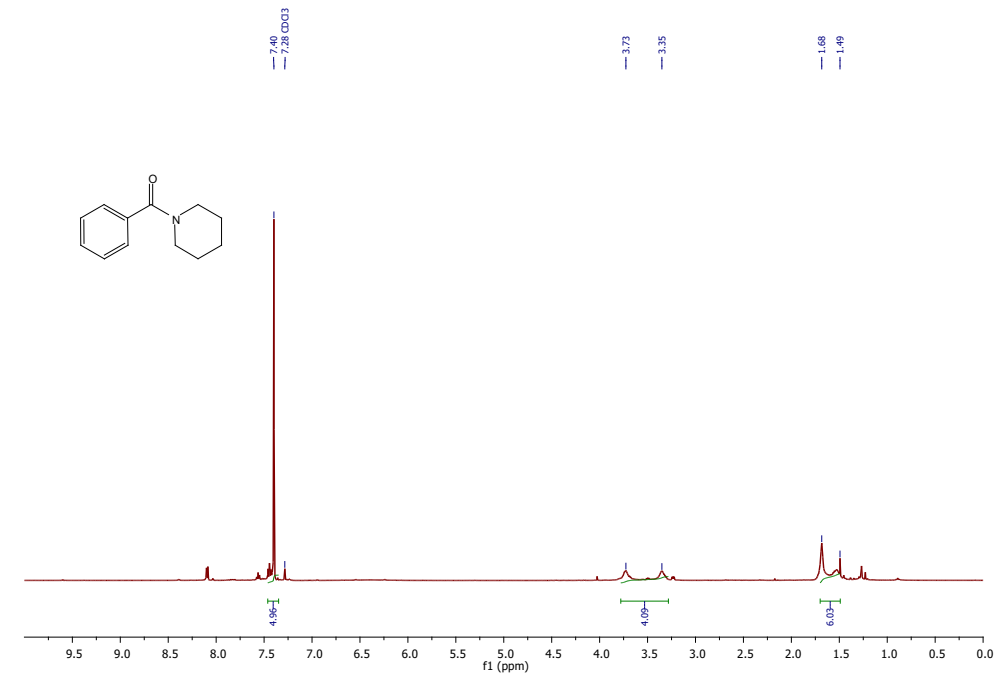

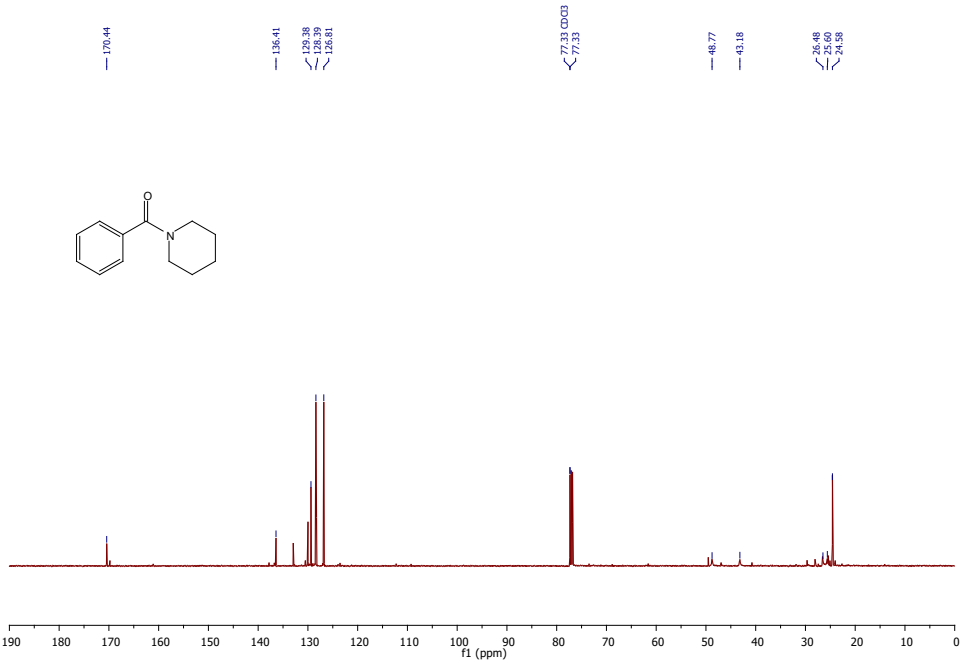

^{1}H and ^{13}C NMR spectra of **3b**

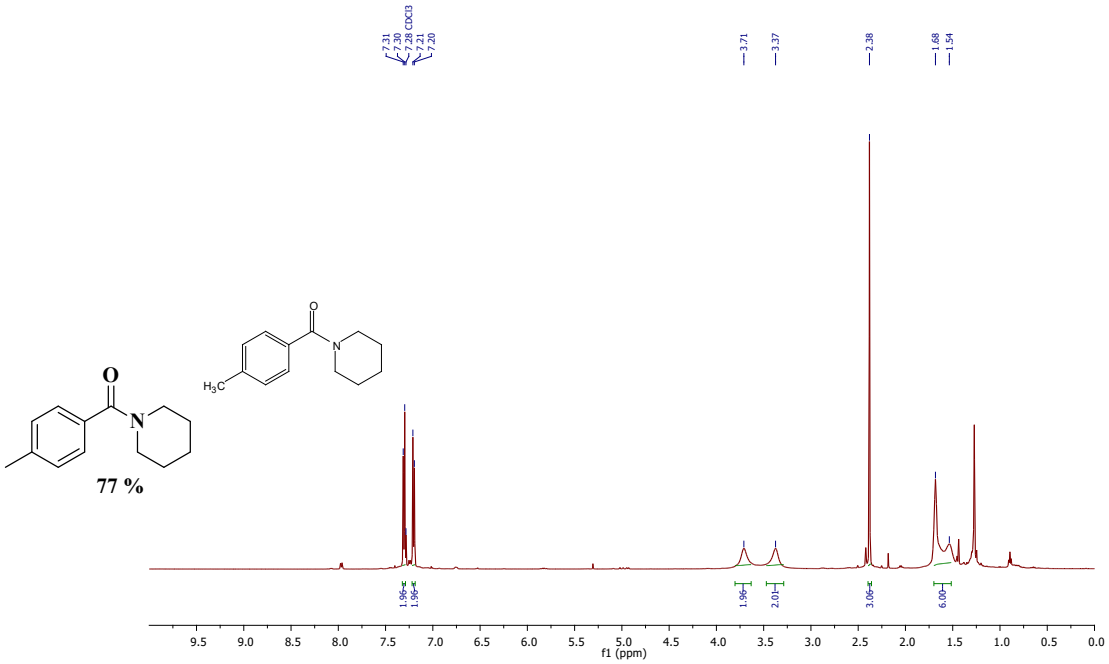

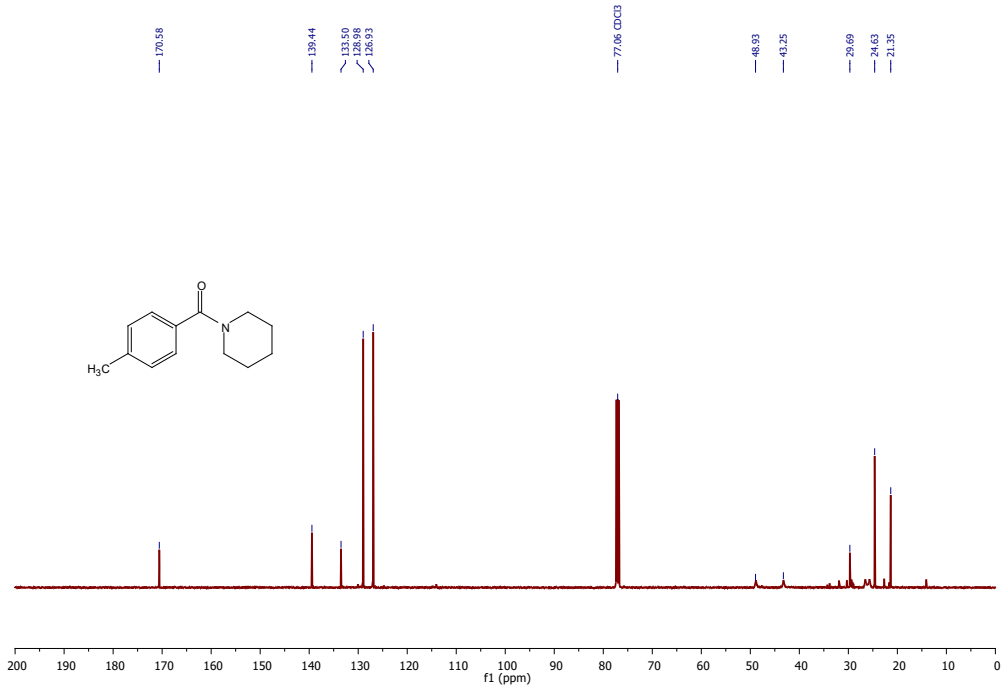

^{1}H and ^{13}C NMR spectra of **3c**

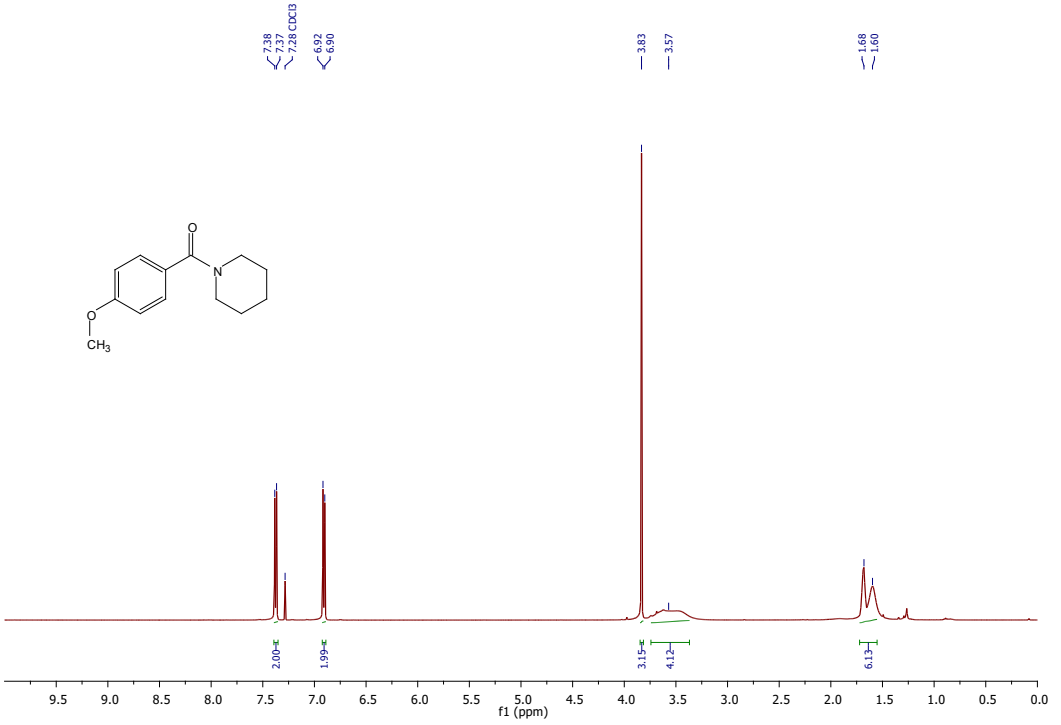

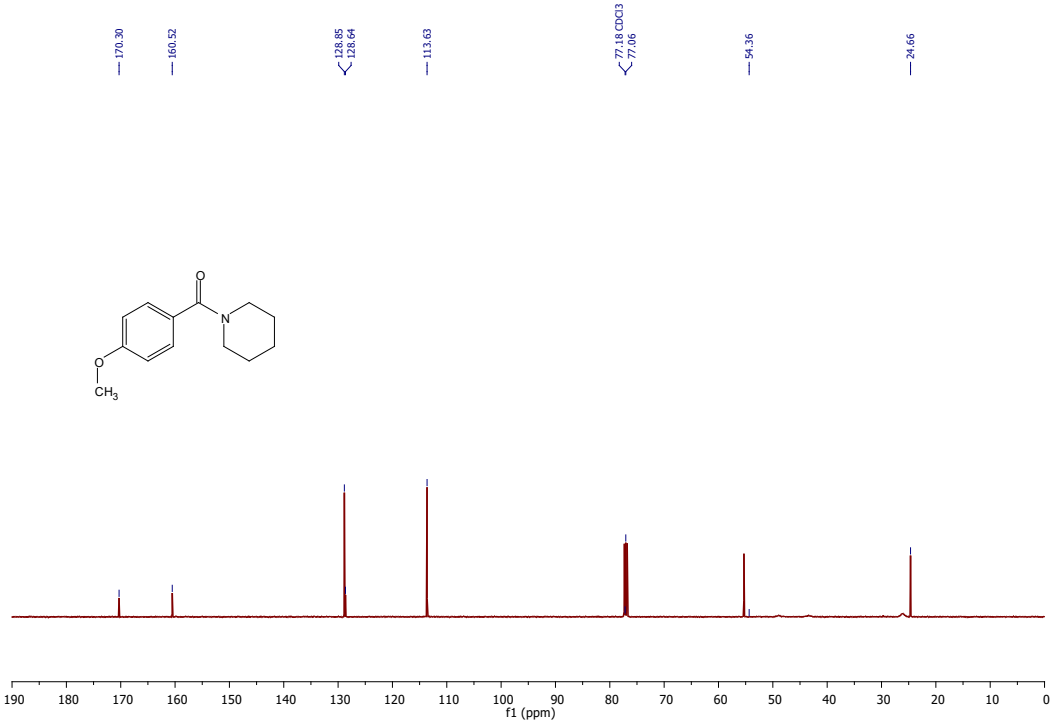

^{1}H and ^{13}C NMR spectra of **3d**

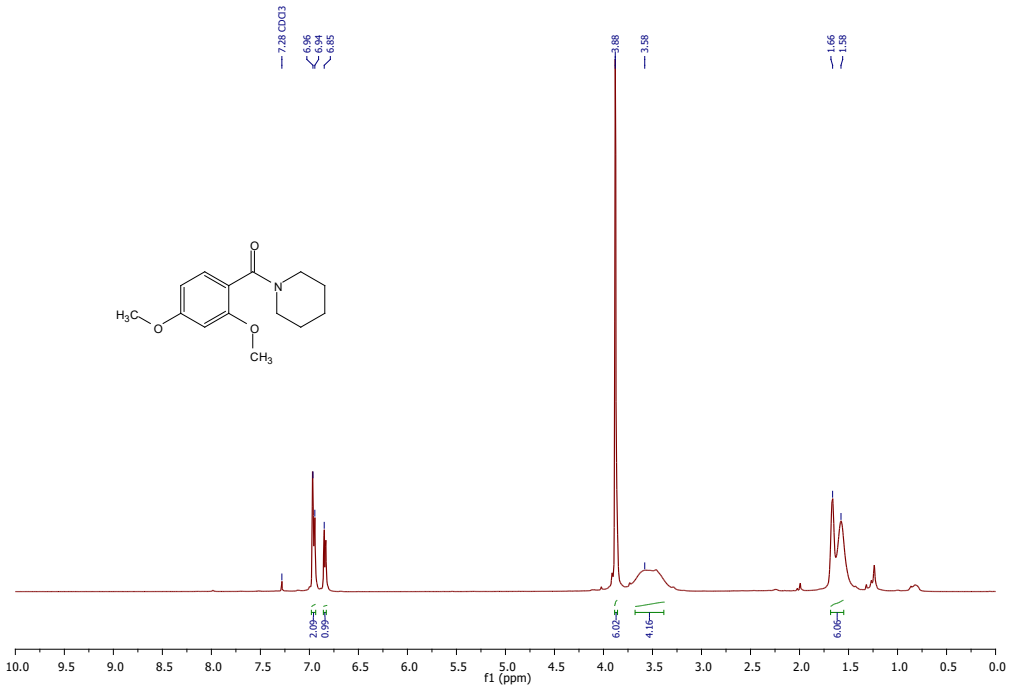

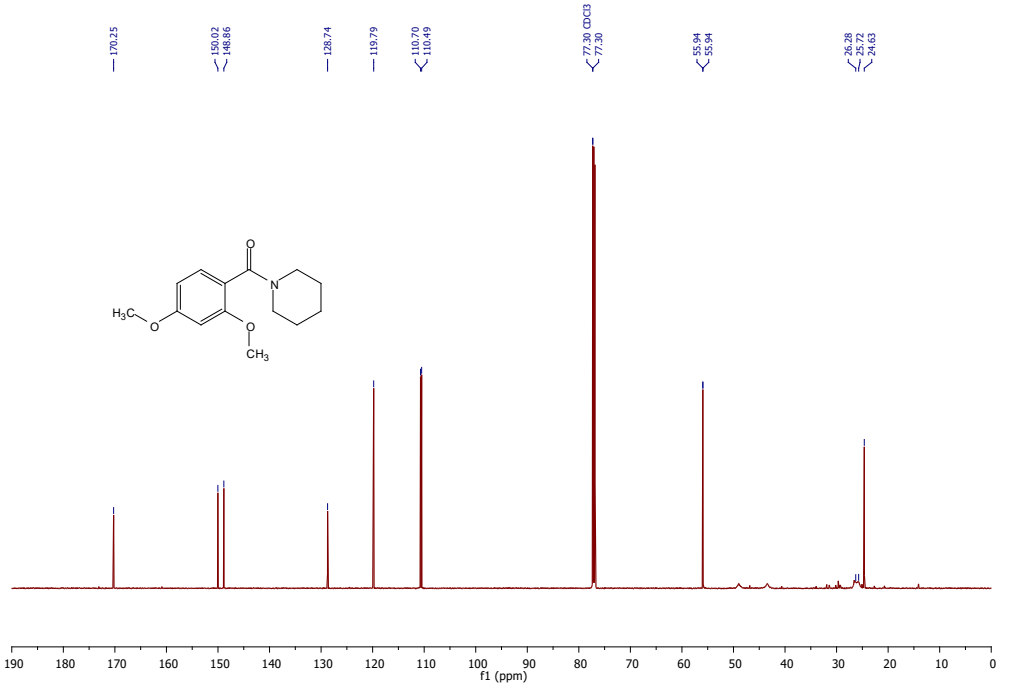

^{1}H and ^{13}C NMR spectra of **3e**

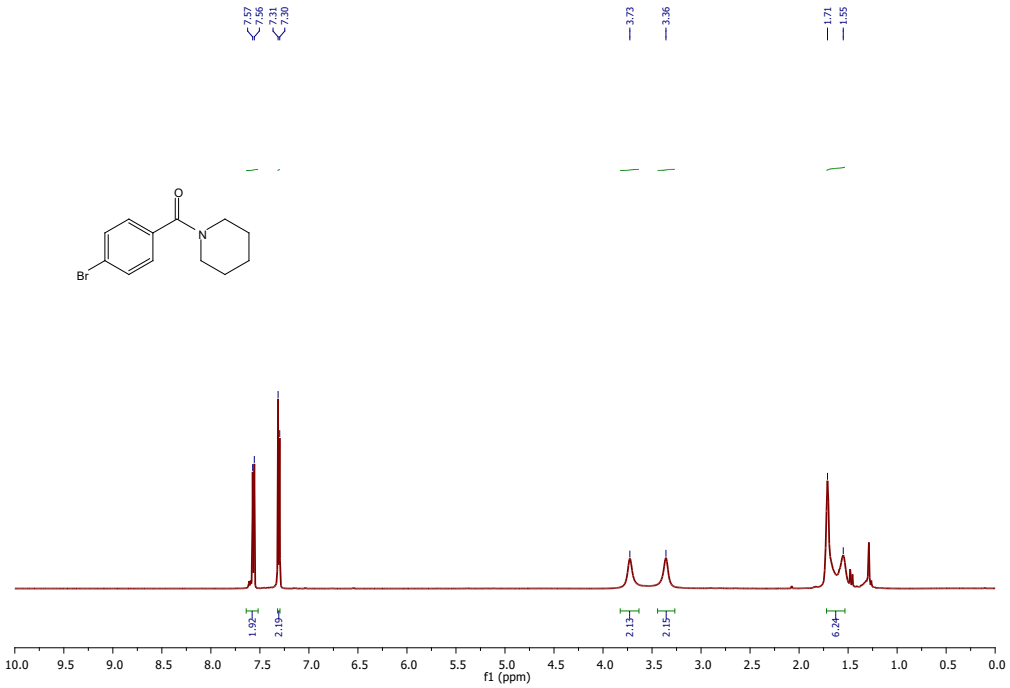

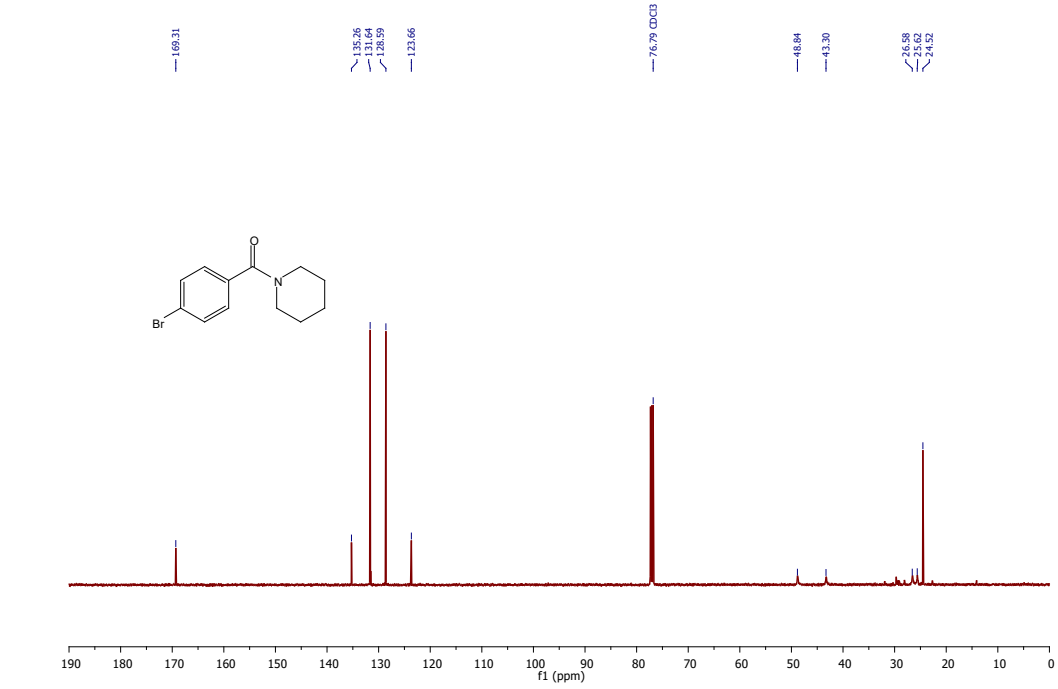

^{1}H and ^{13}C NMR spectra of **3f**

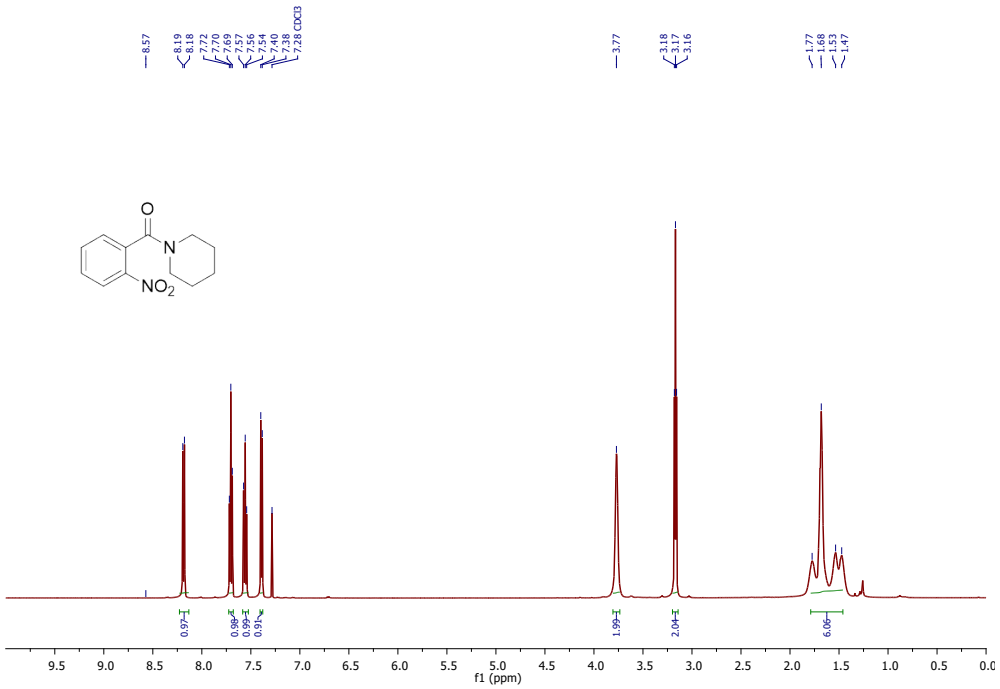

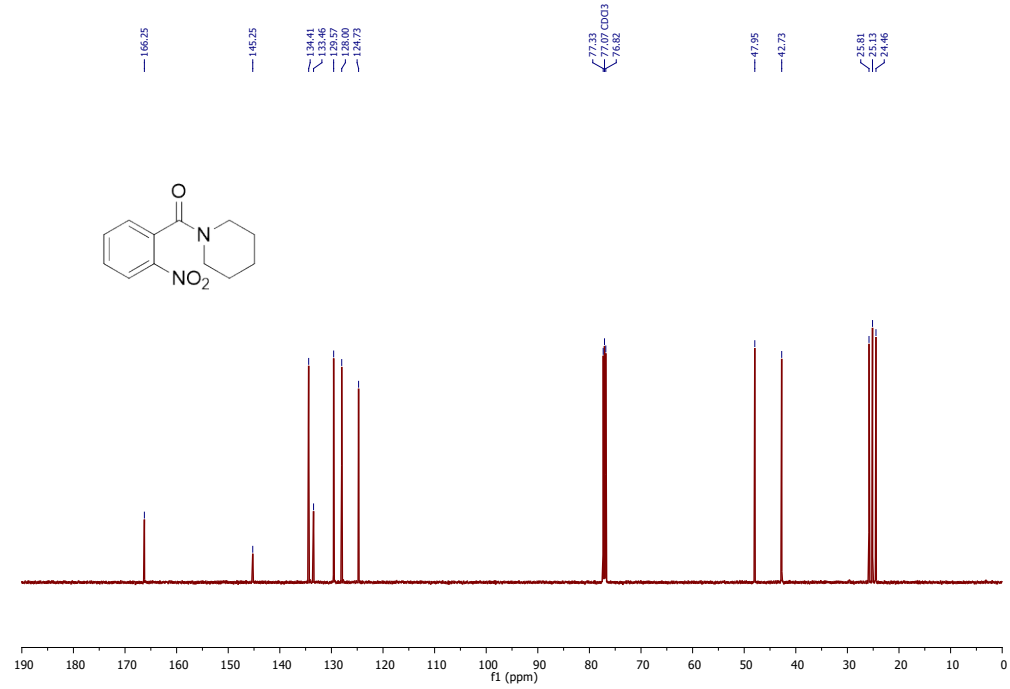

^{1}H and ^{13}C NMR spectra of **3g**

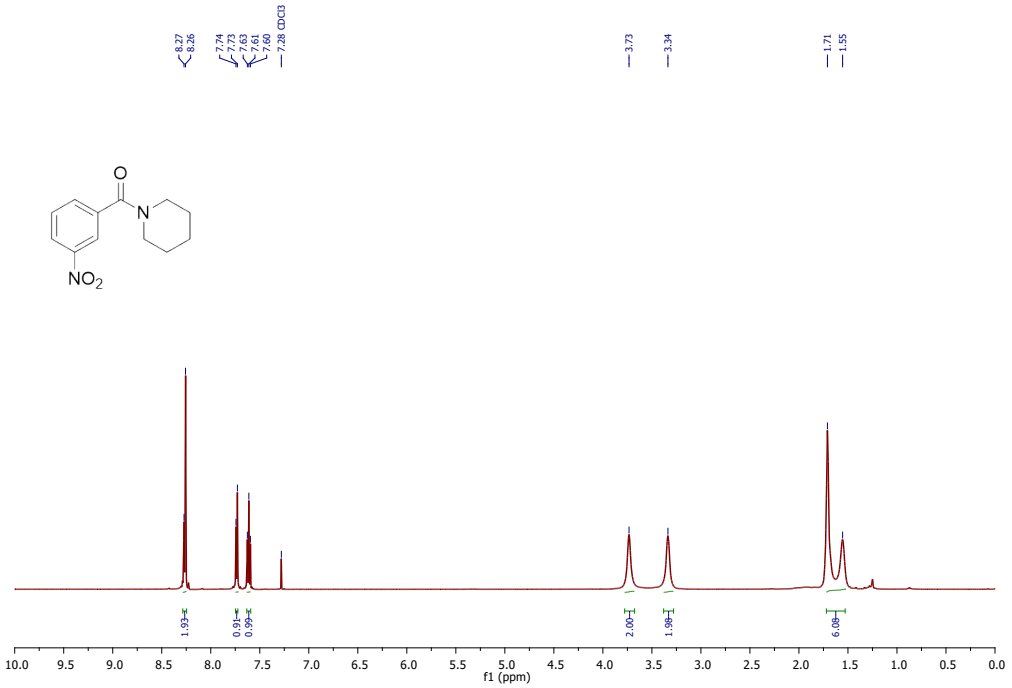

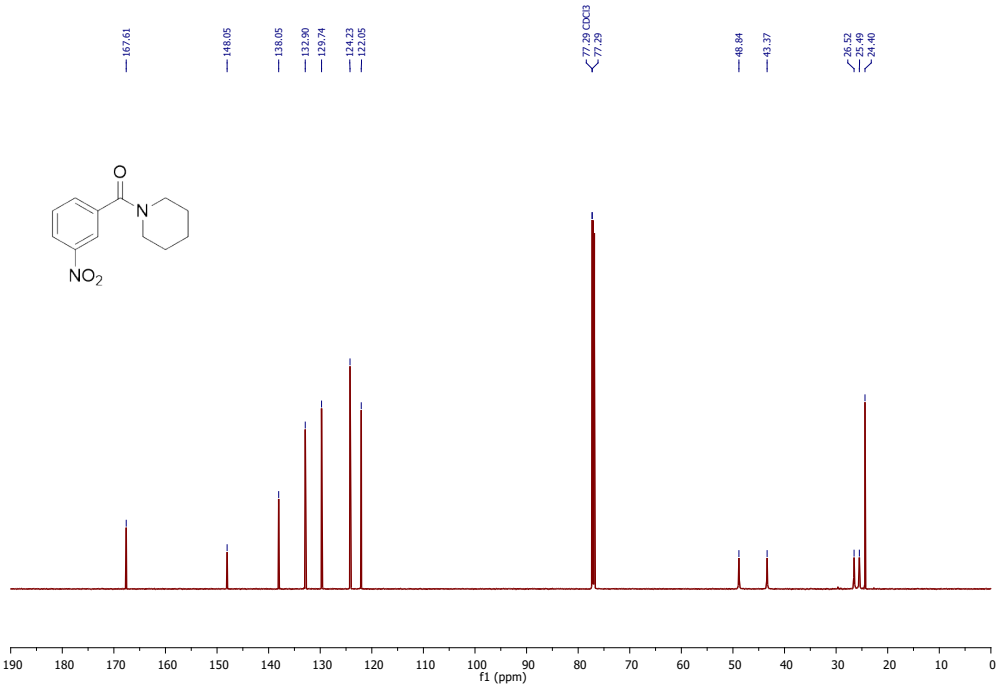

^{1}H and ^{13}C NMR spectra of **3h**

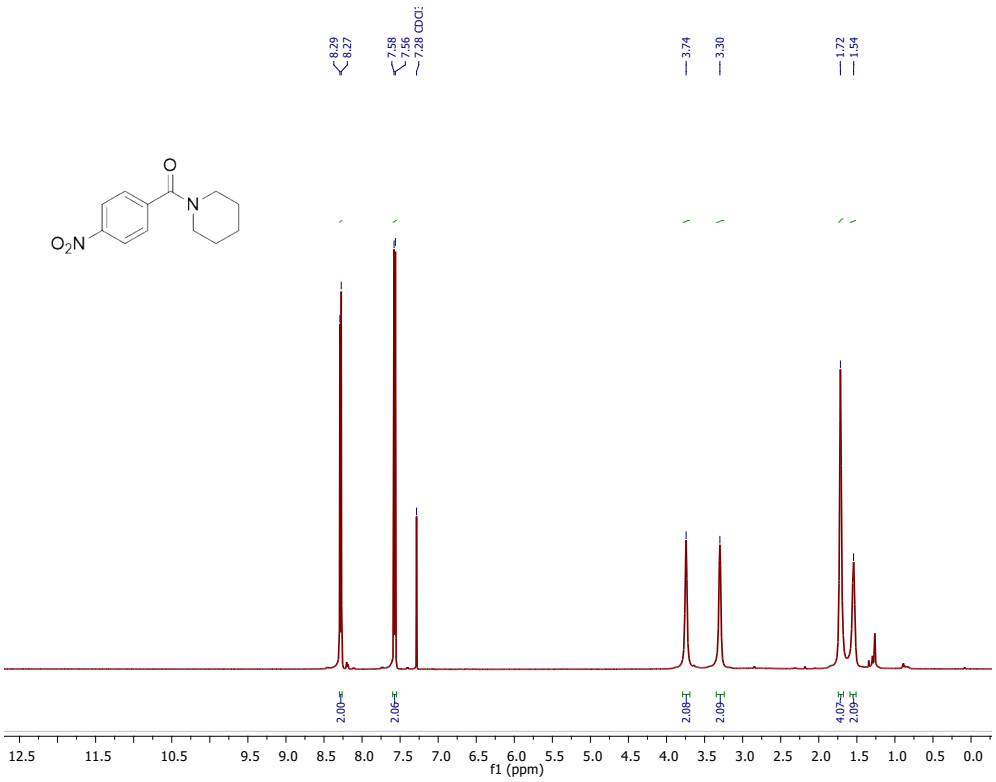

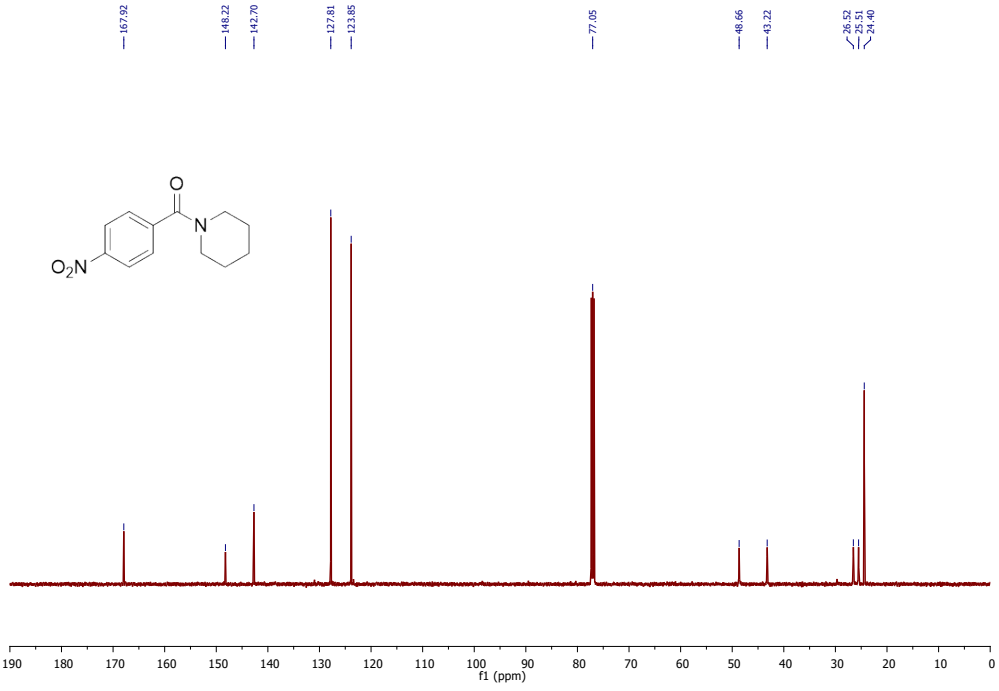

^{1}H and ^{13}C NMR spectra of **3i**

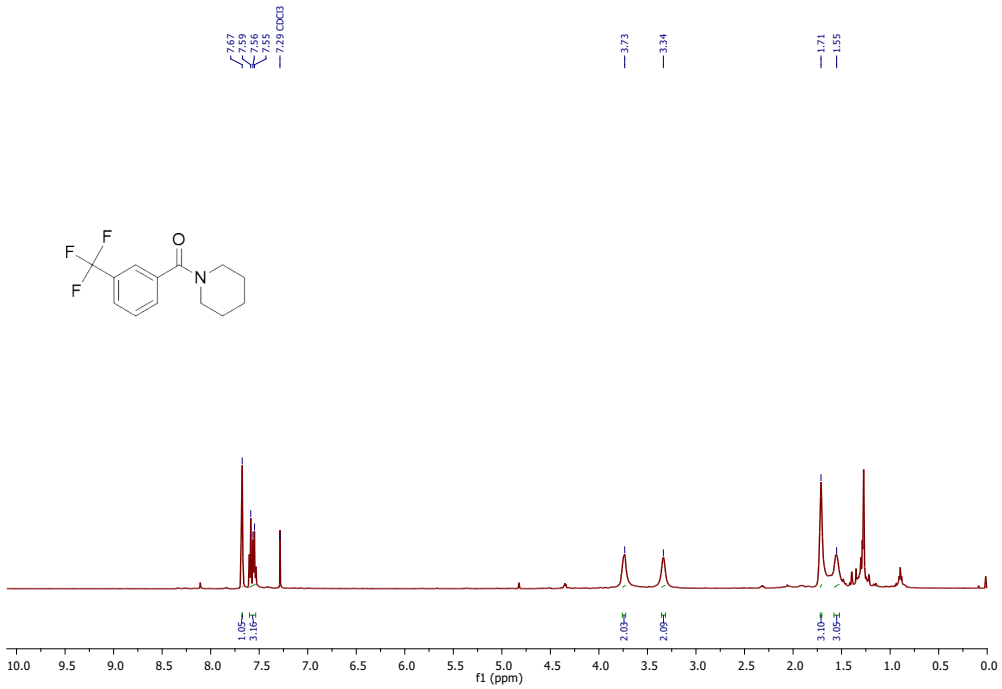

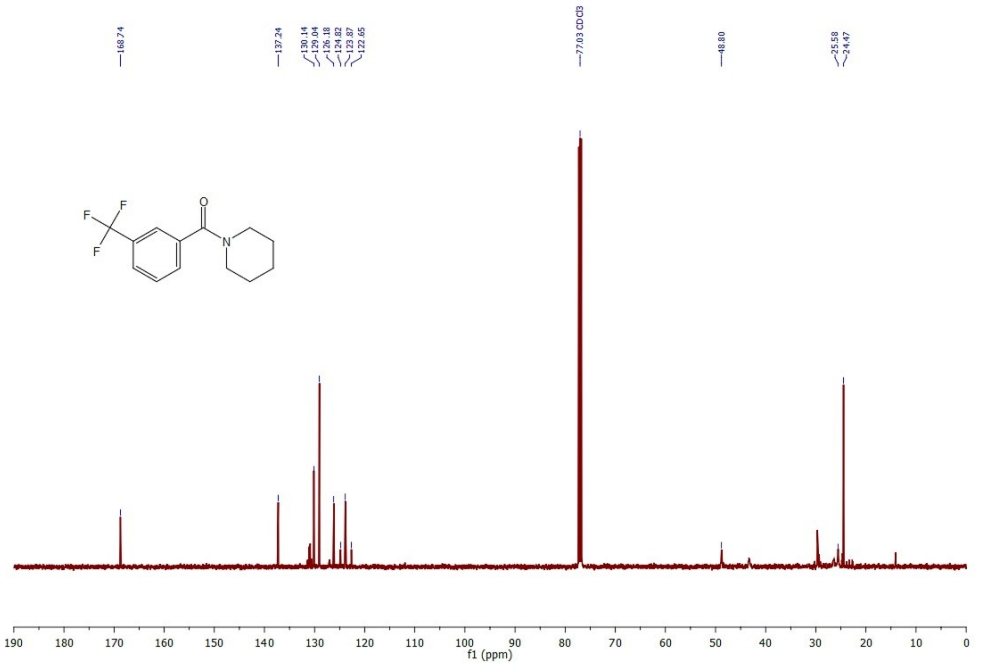

^{1}H and ^{13}C NMR spectra of **3j**

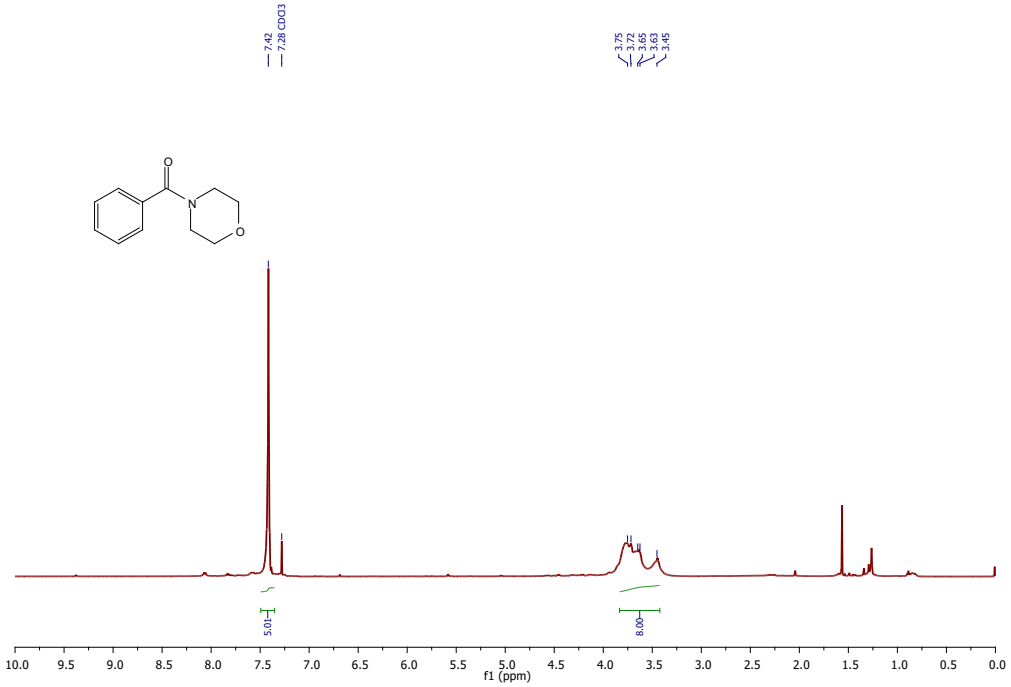

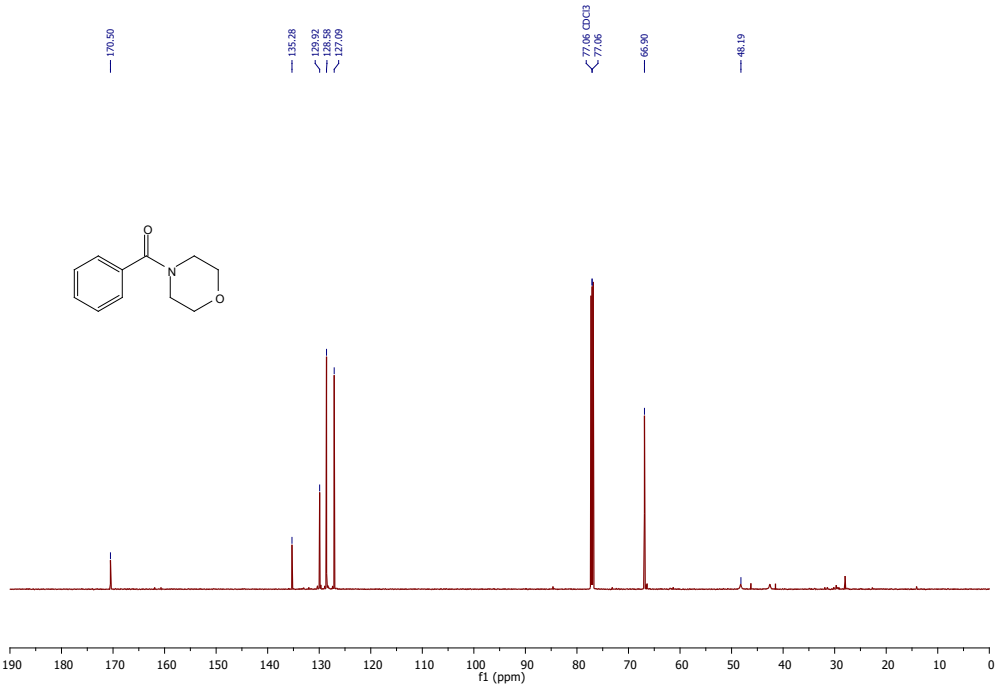

^{1}H and ^{13}C NMR spectra of **3k**

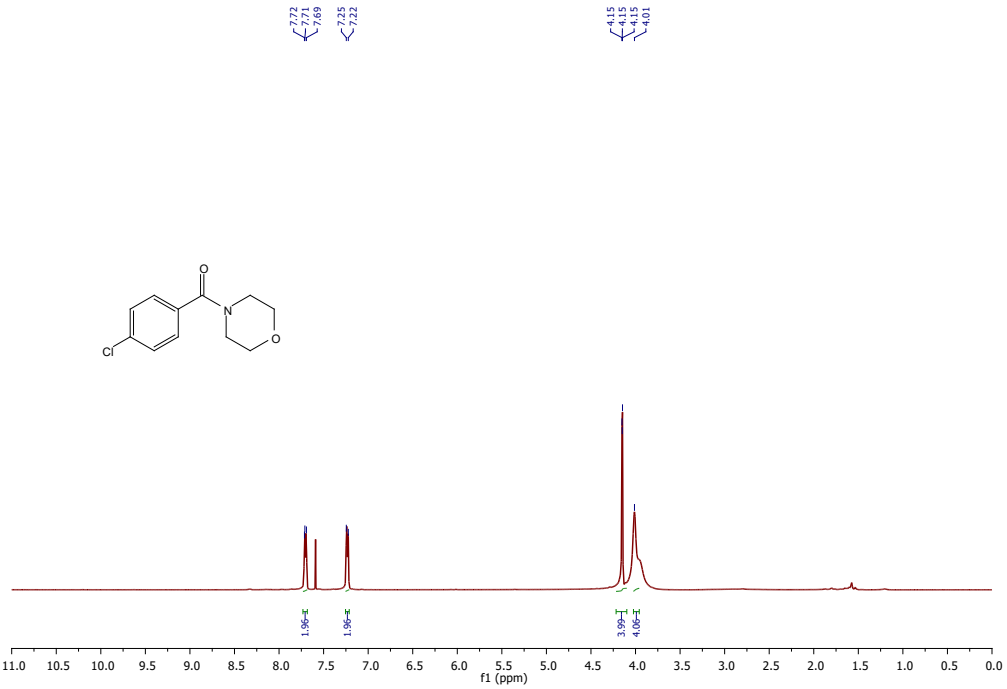

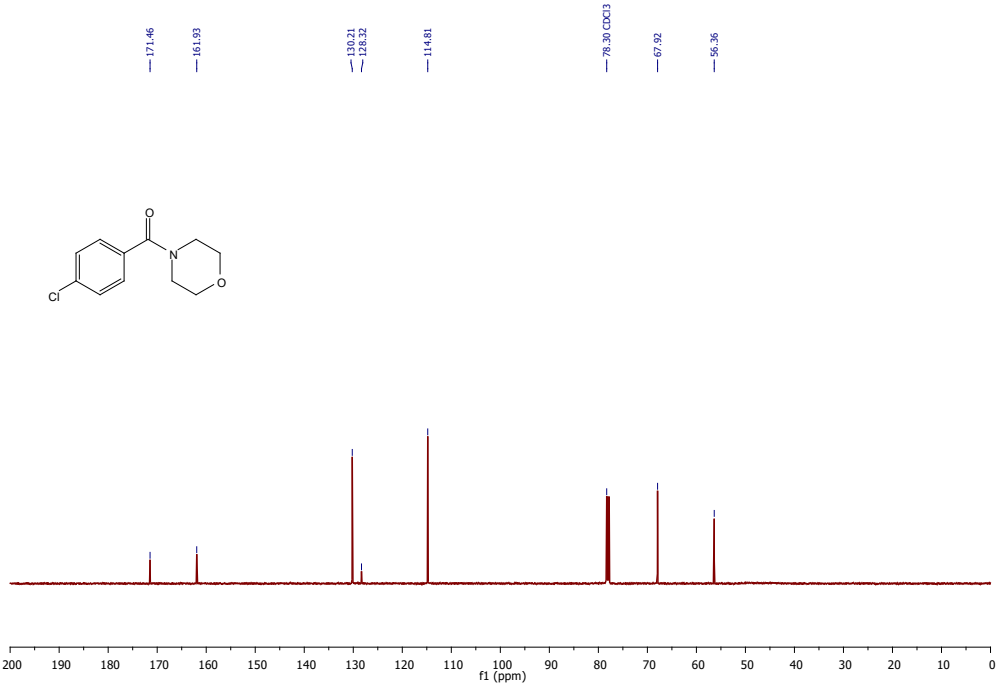

^{1}H and ^{13}C NMR spectra of **3l**

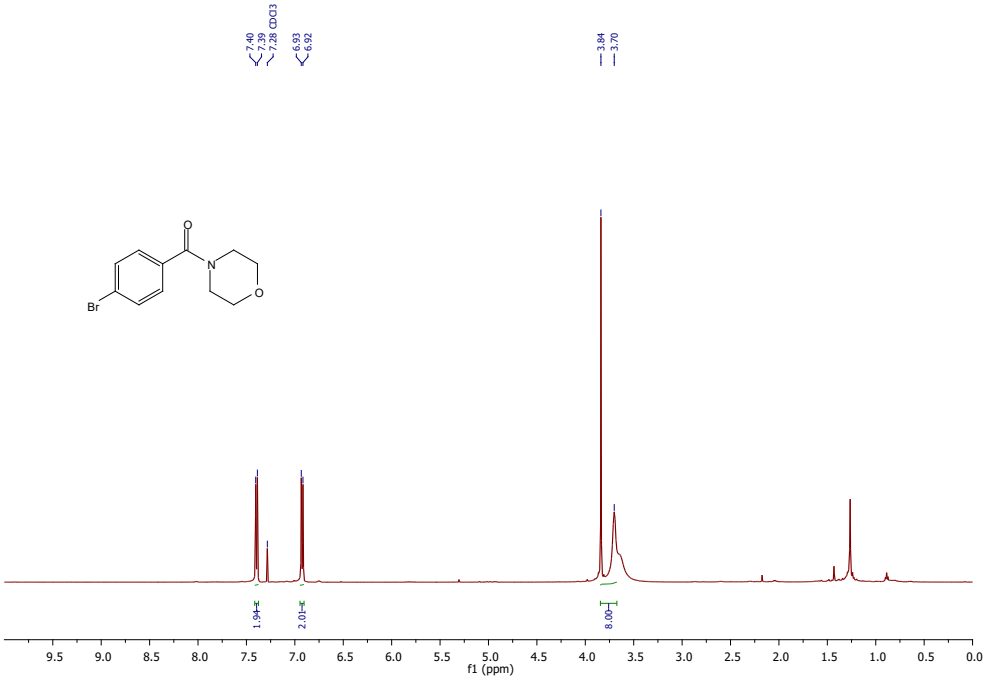

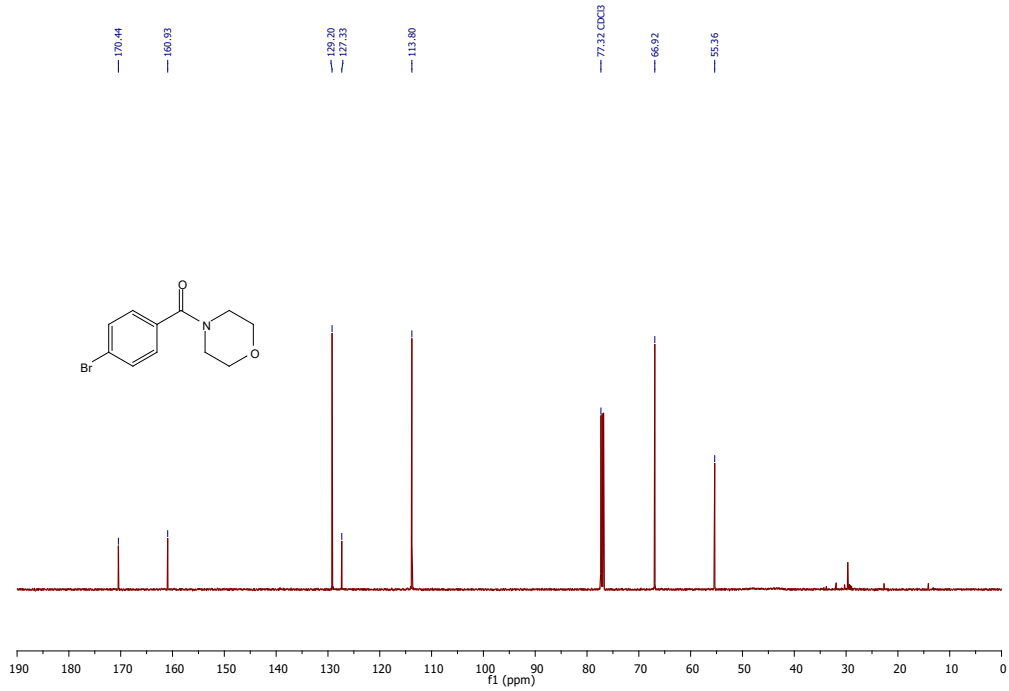

^{1}H and ^{13}C NMR spectra of **3m**

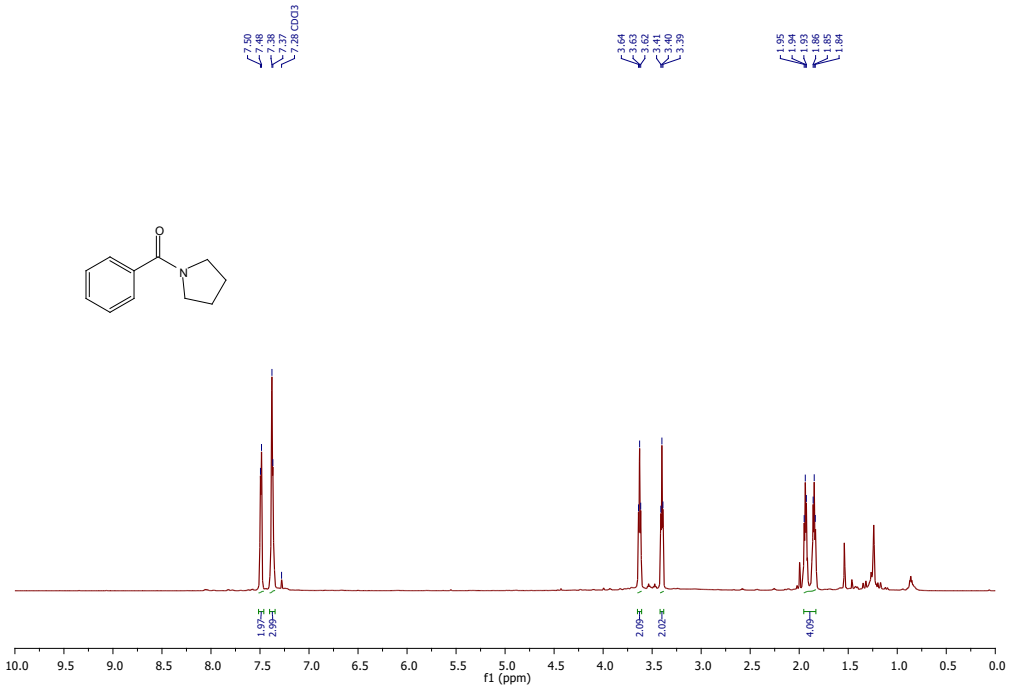

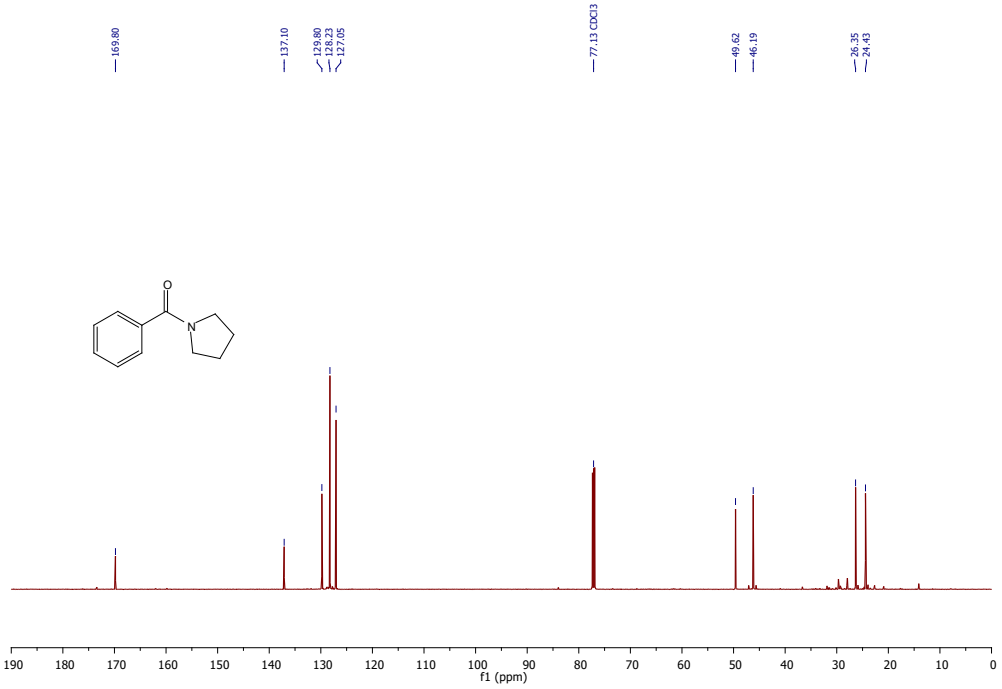

^{1}H and ^{13}C NMR spectra of **3n**

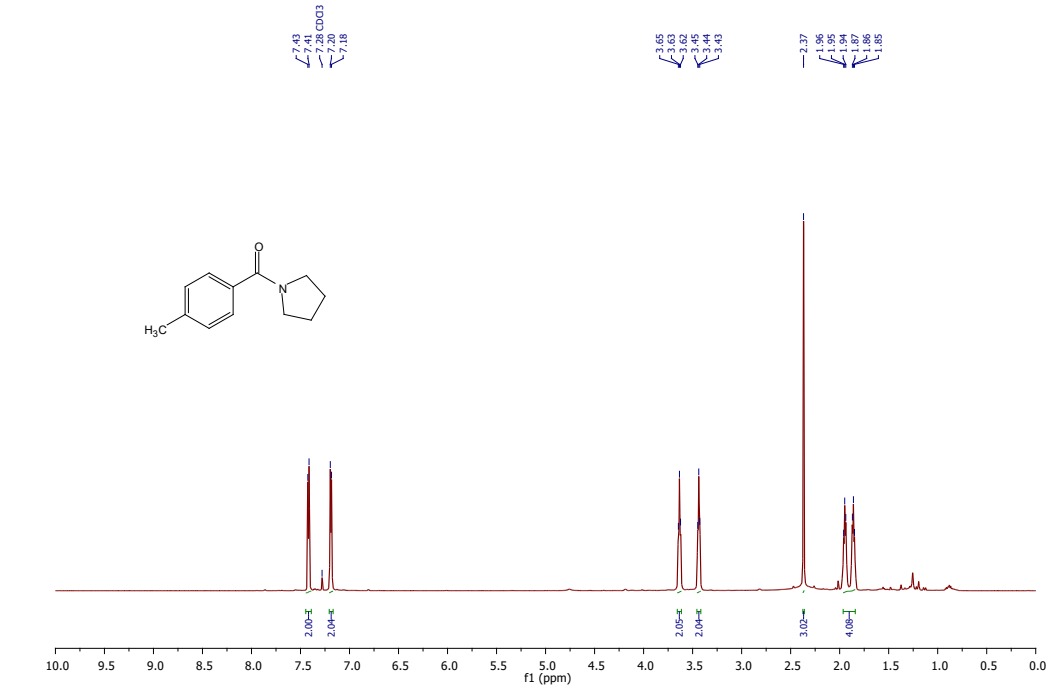

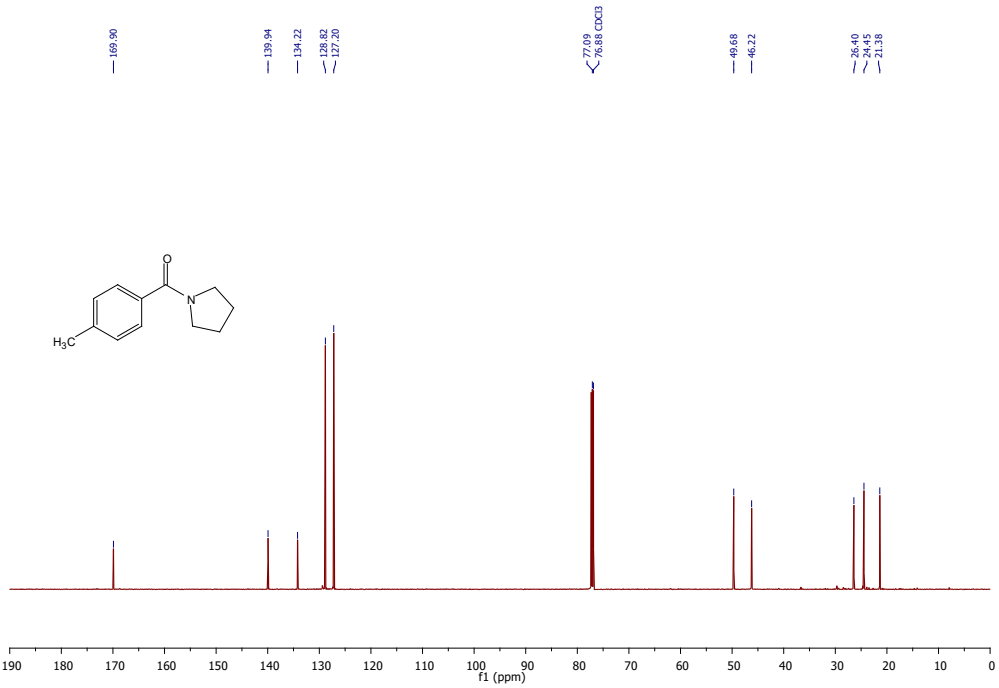

^{1}H and ^{13}C NMR spectra of **3o**

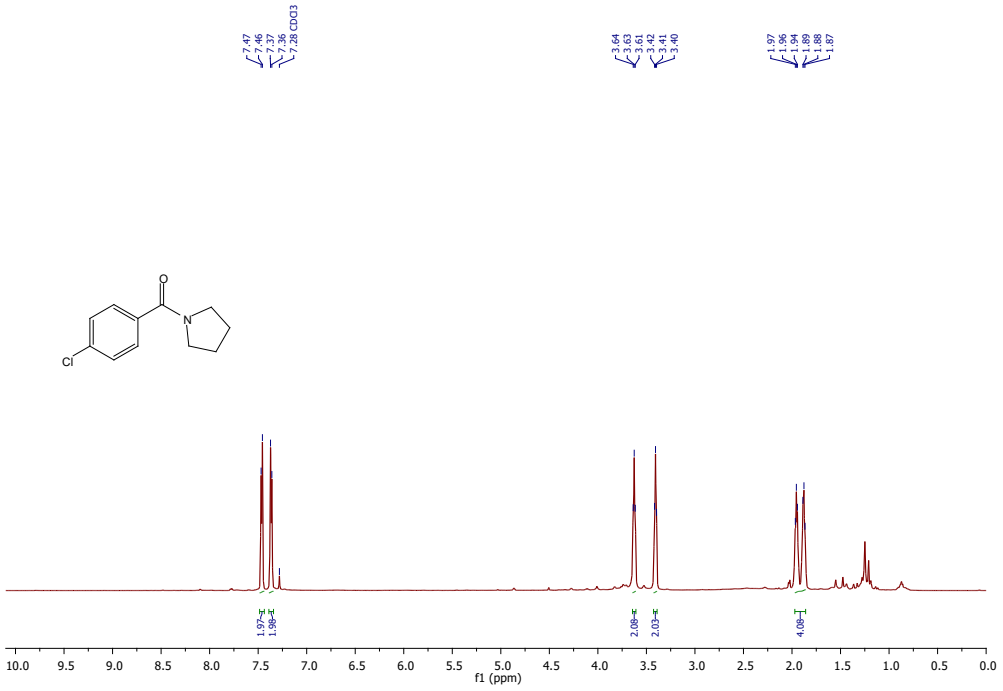

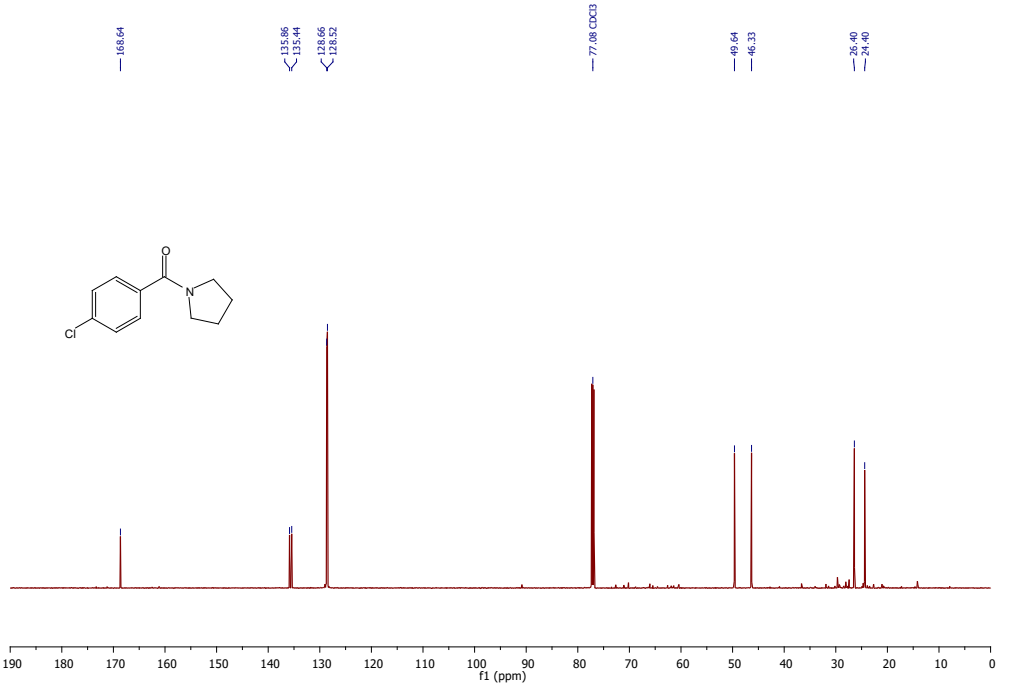

^{1}H and ^{13}C NMR spectra of **3p**

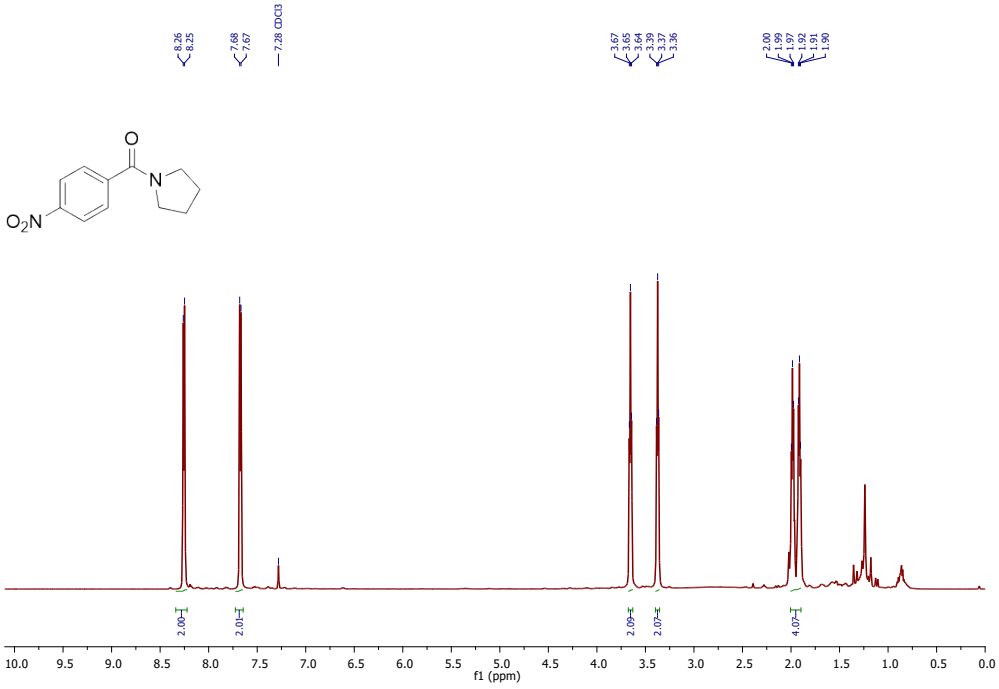

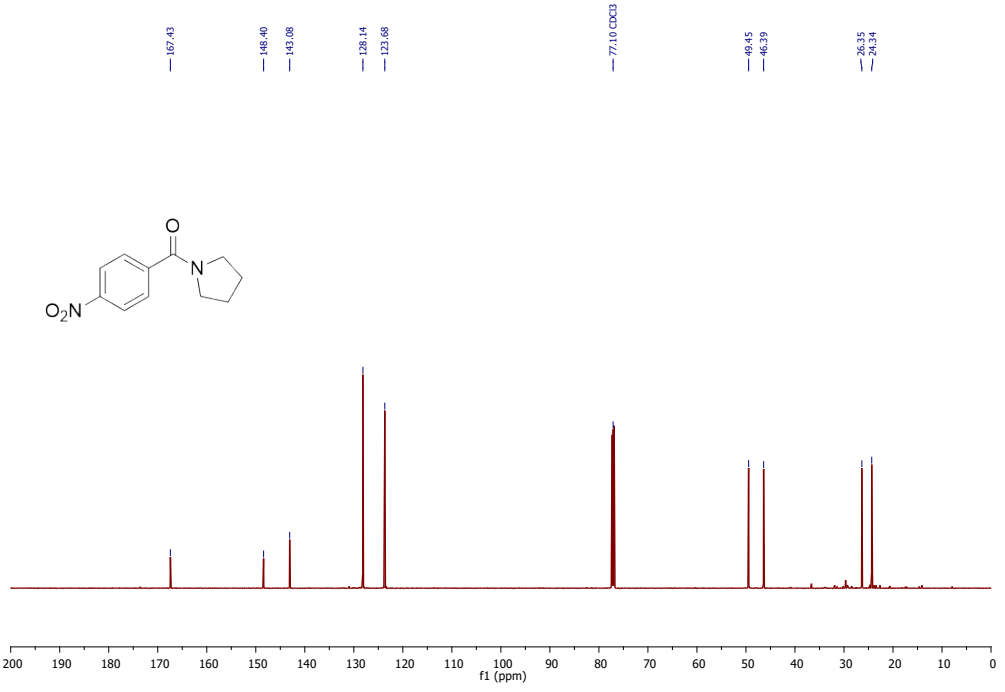

^{1}H and ^{13}C NMR spectra of **3q**

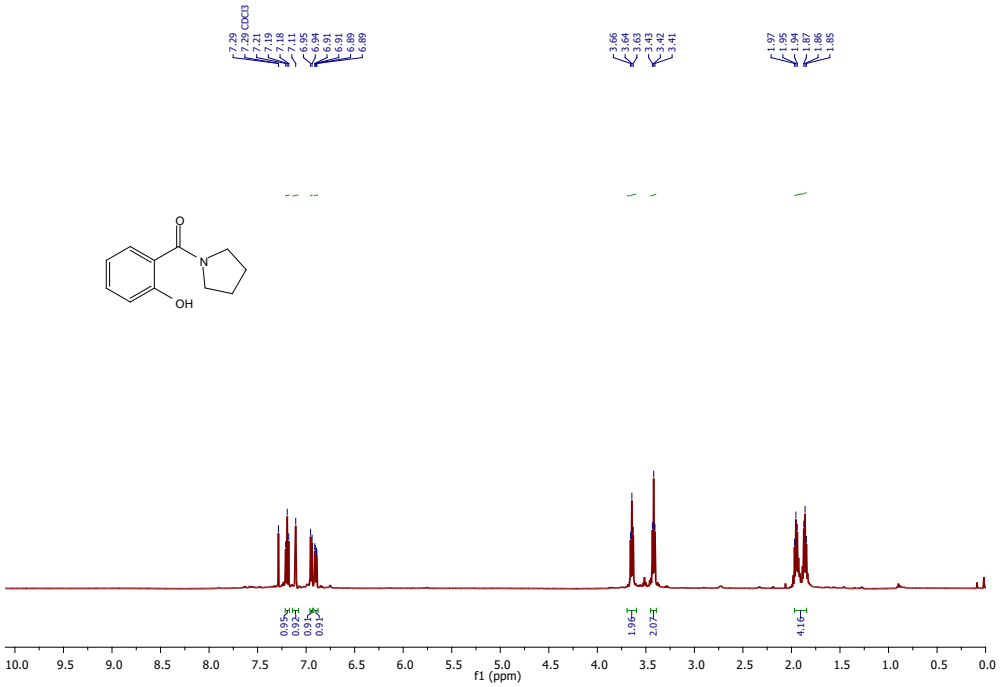

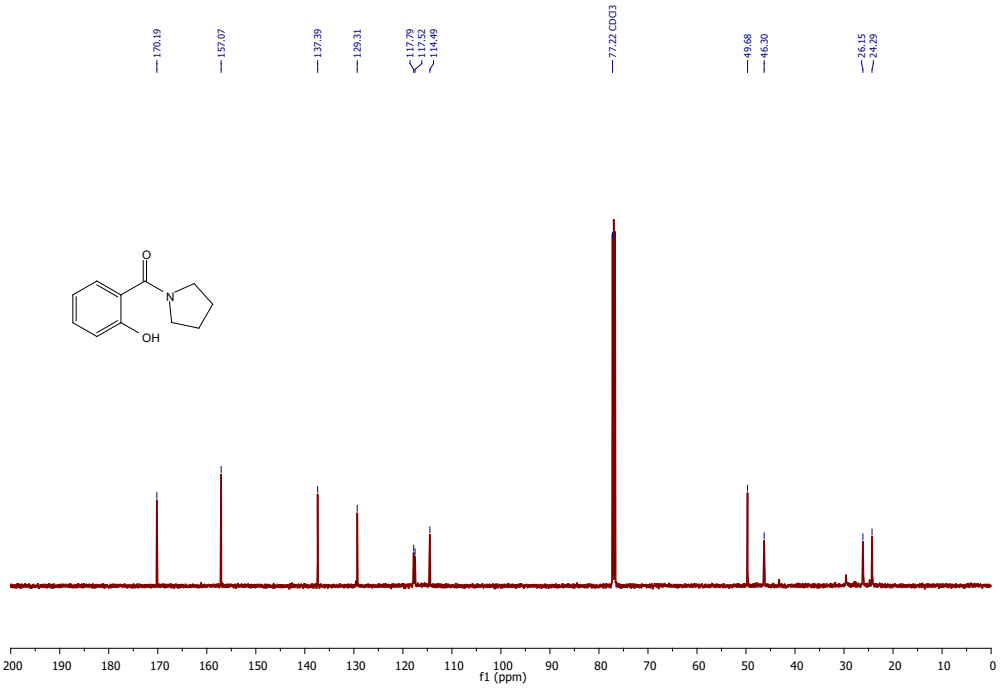

^{1}H and ^{13}C NMR spectra of **3r**

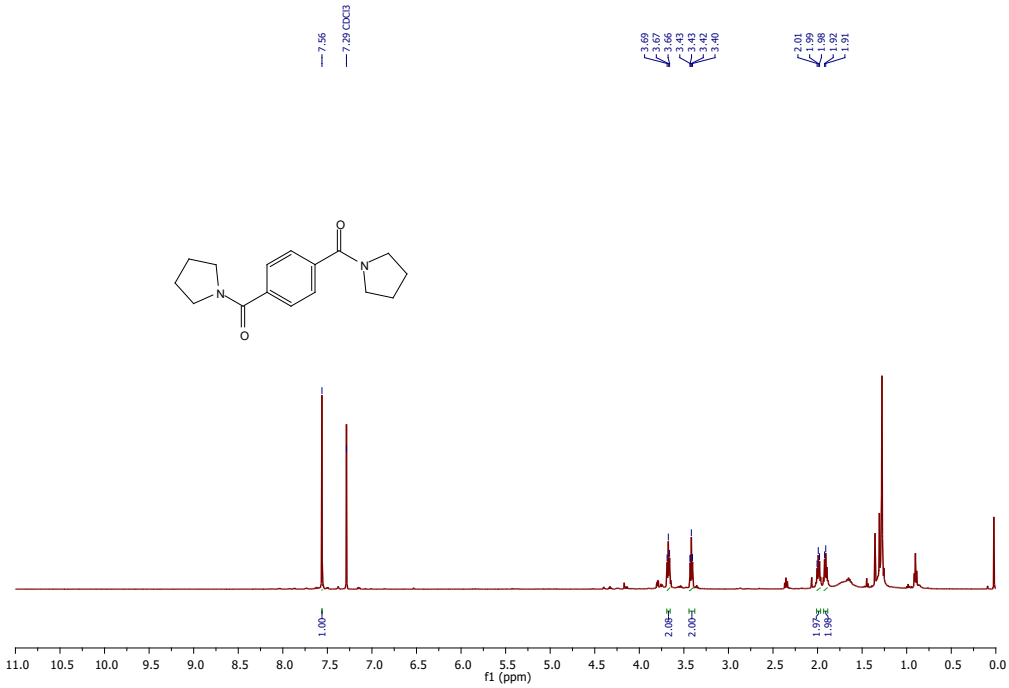

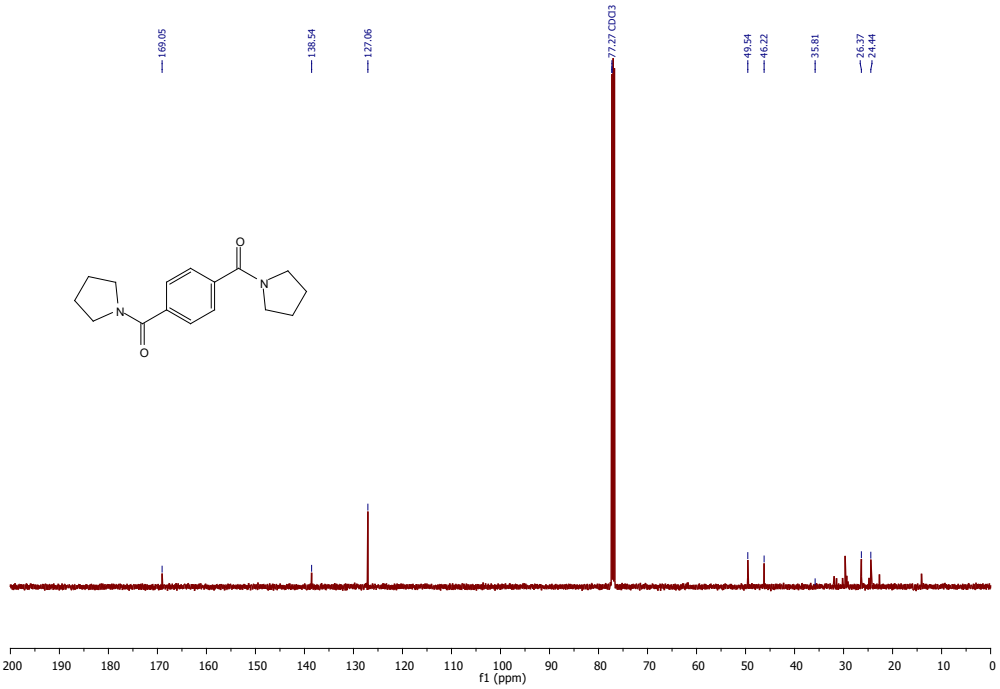

^{1}H and ^{13}C NMR spectra of **3s**

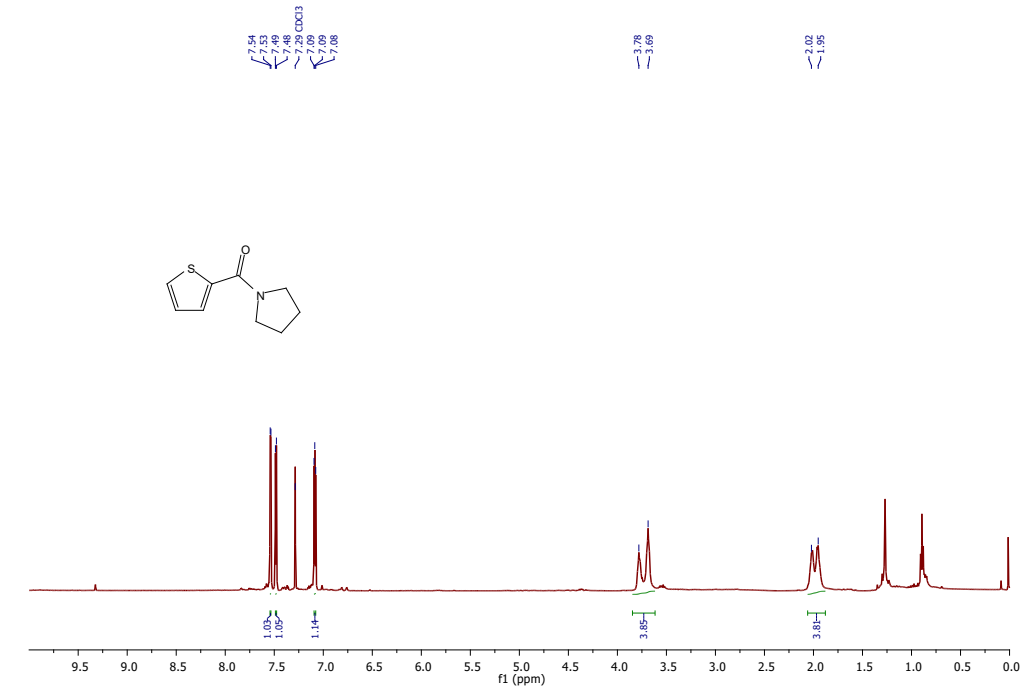

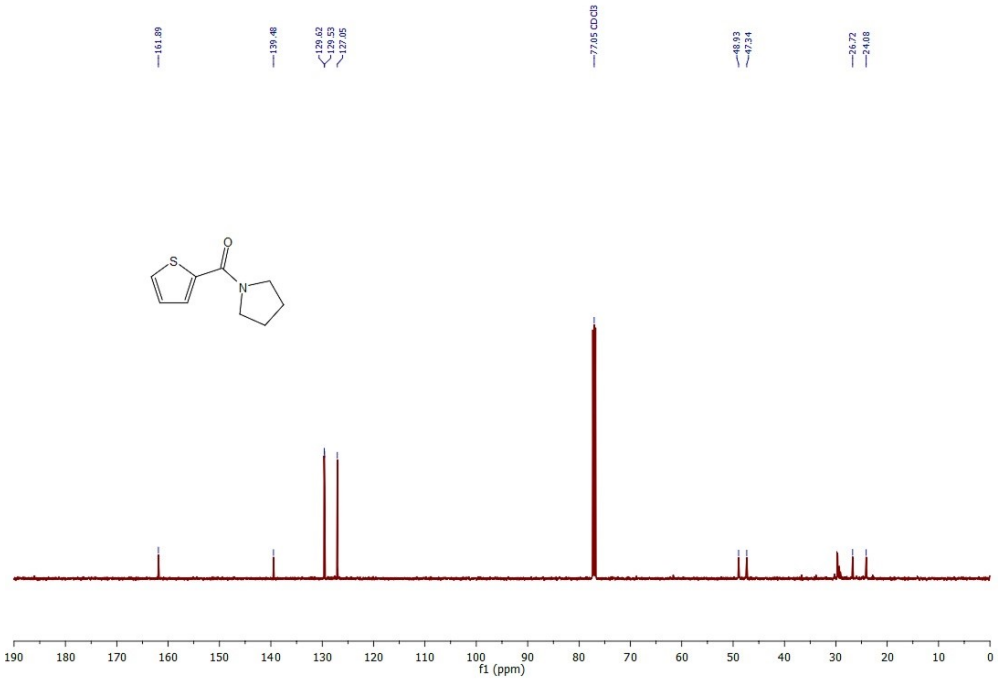

^{1}H and ^{13}C NMR spectra of **3t**

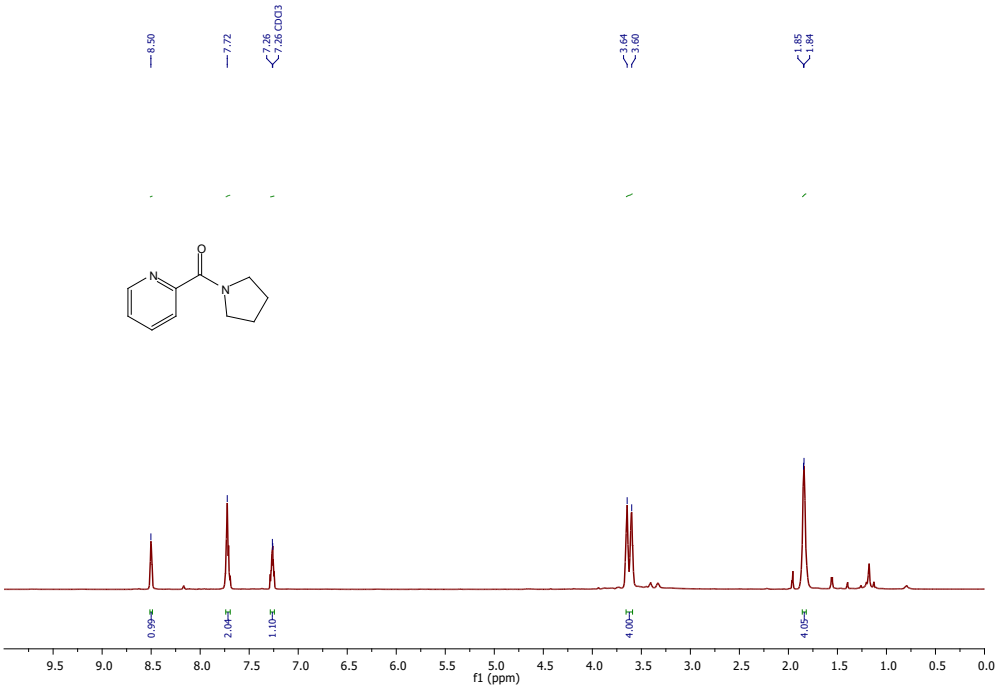

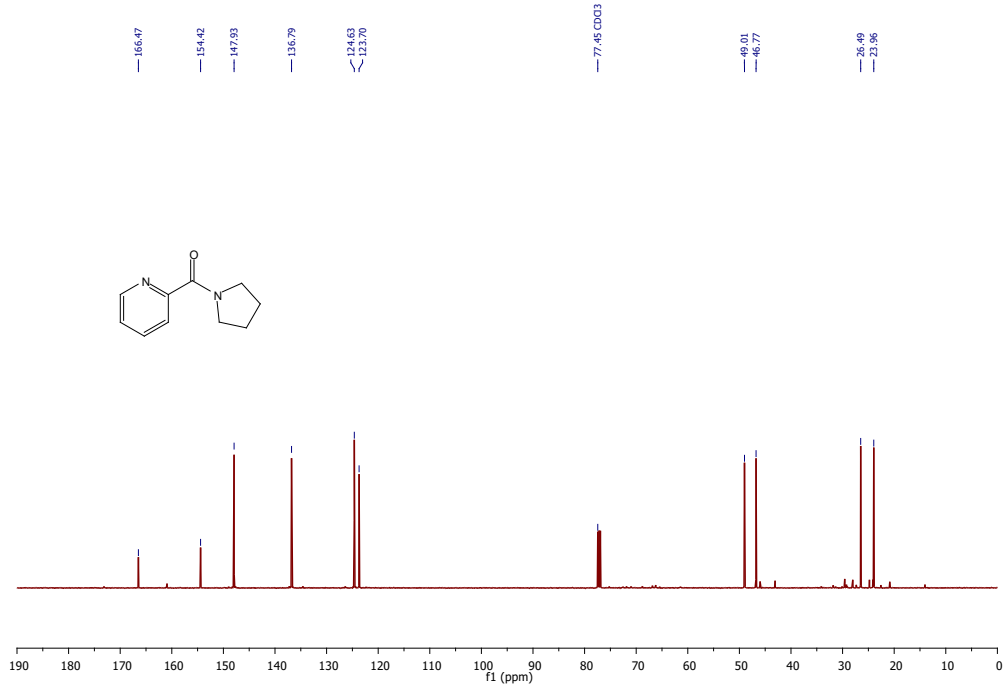

^{1}H and ^{13}C NMR spectra of **3u**

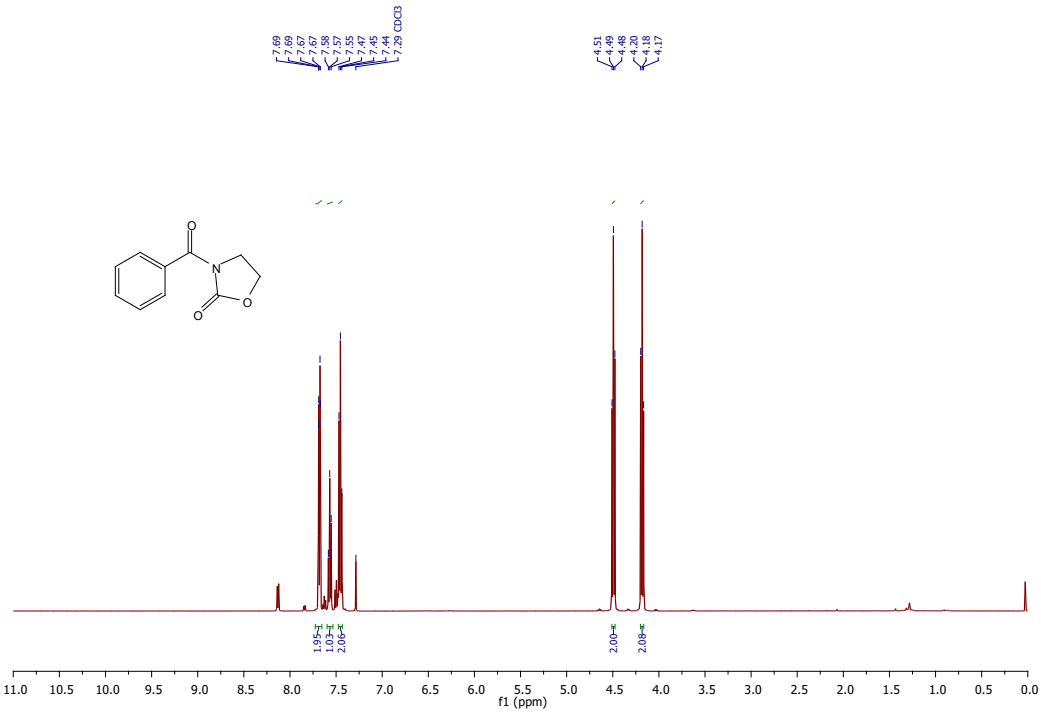

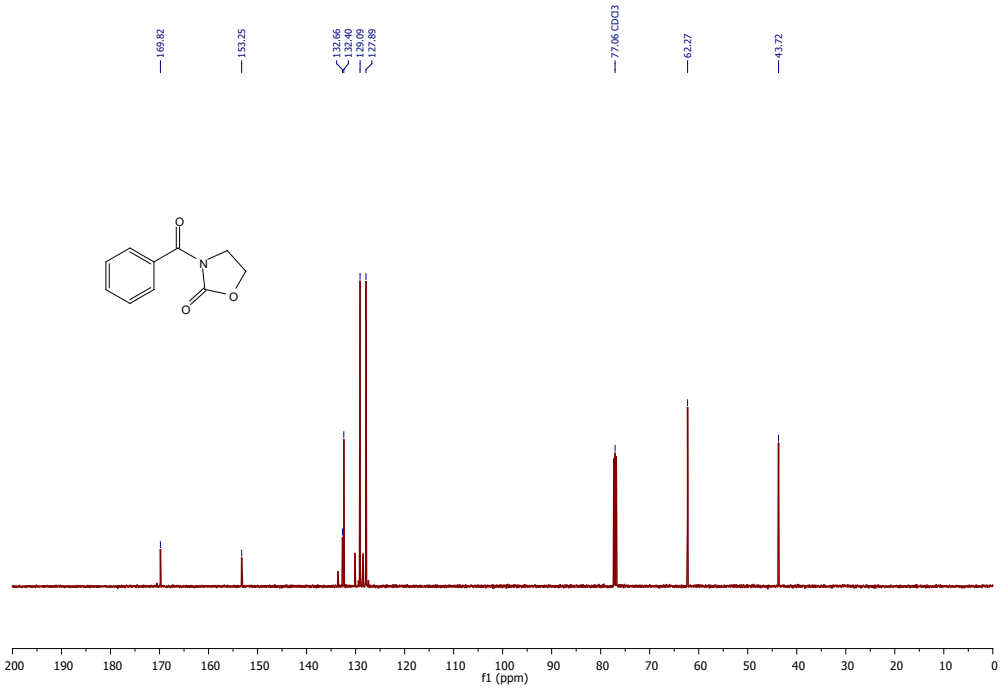

^{1}H and ^{13}C NMR spectra of **3v**

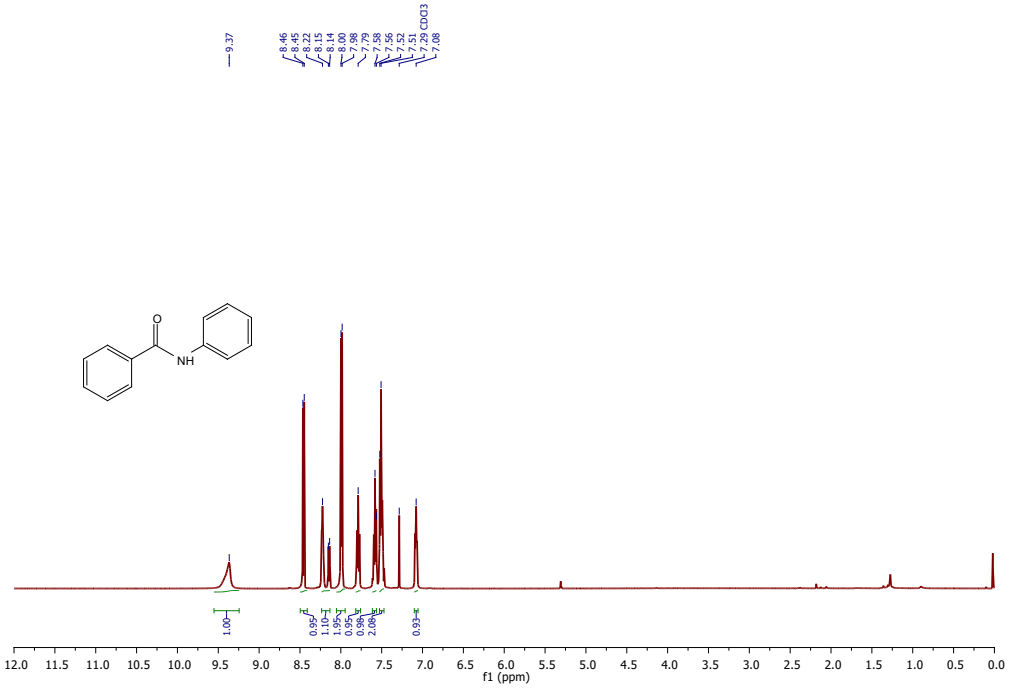

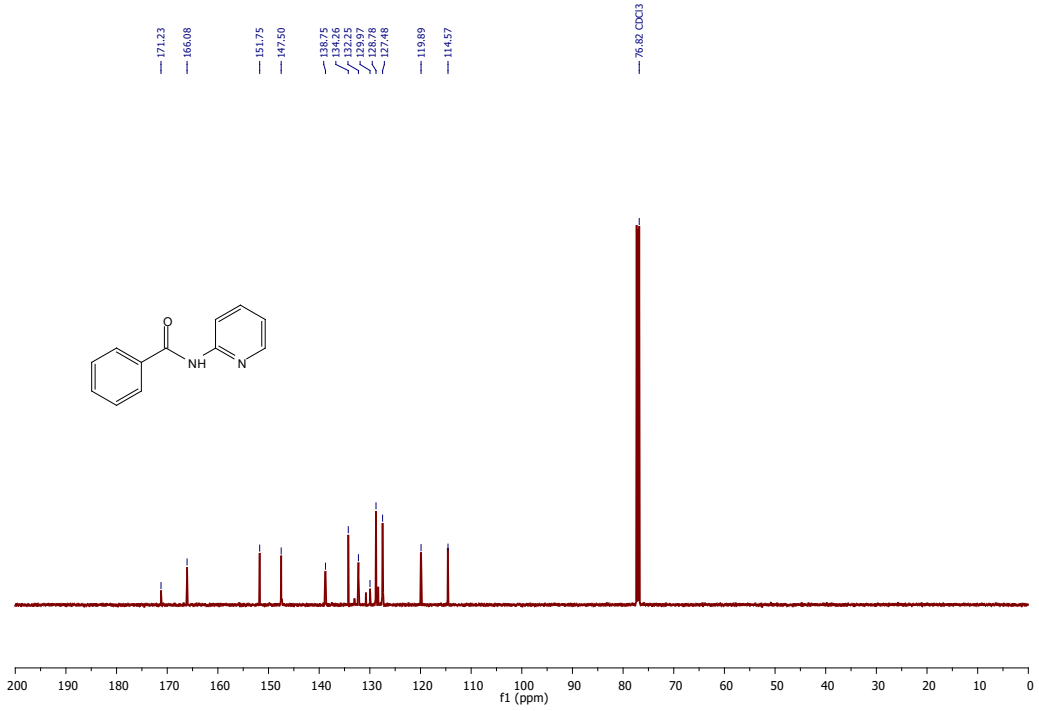

^{1}H and ^{13}C NMR spectra of **3w**

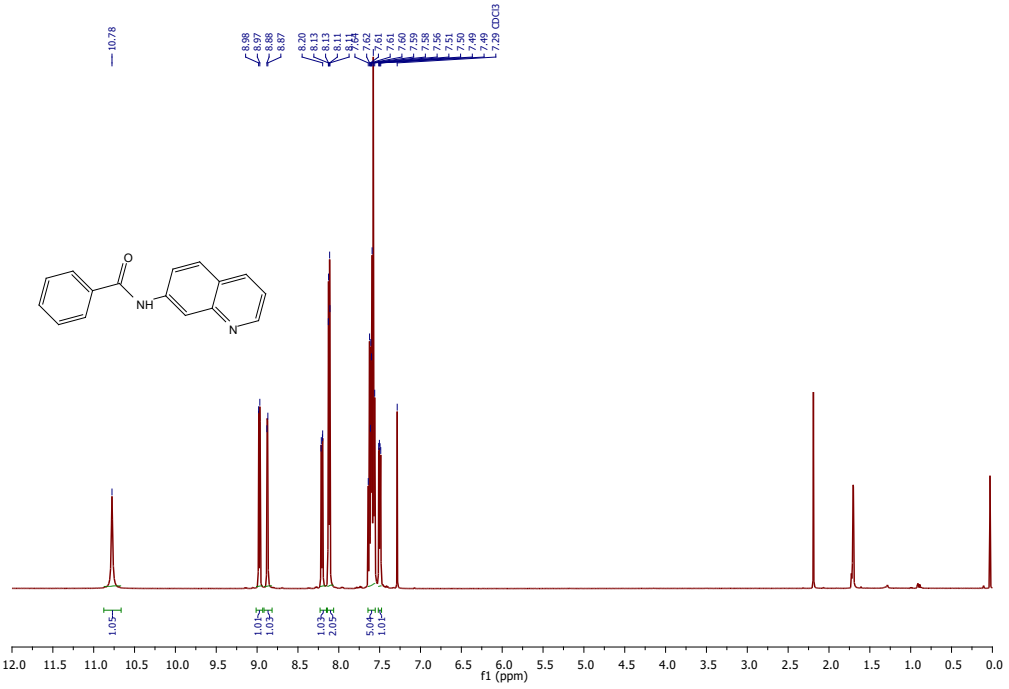

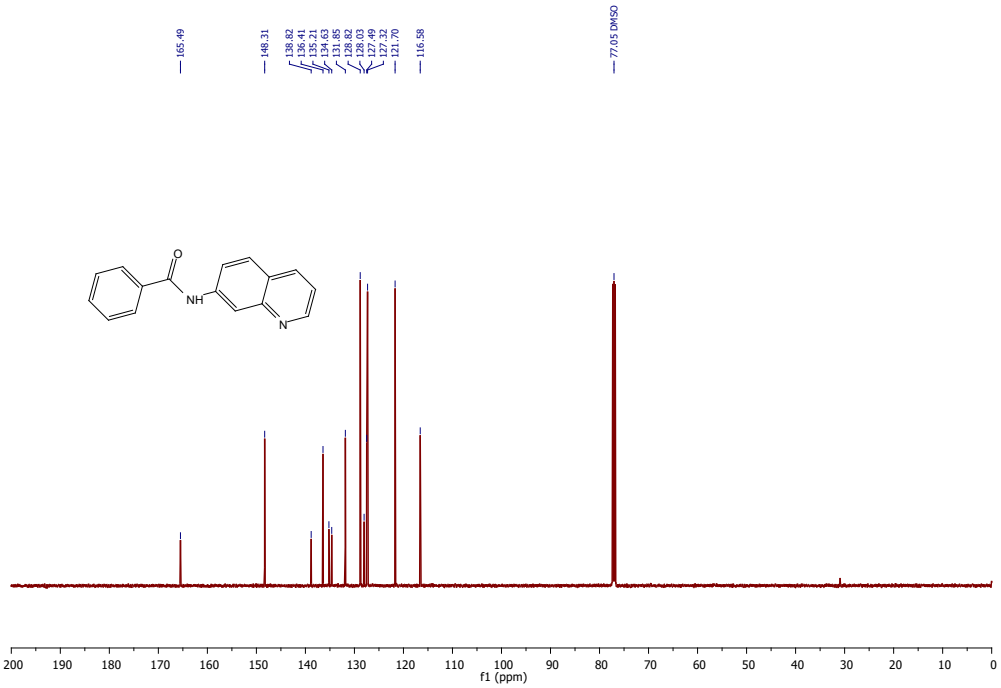

^{1}H and ^{13}C NMR spectra of **3x**

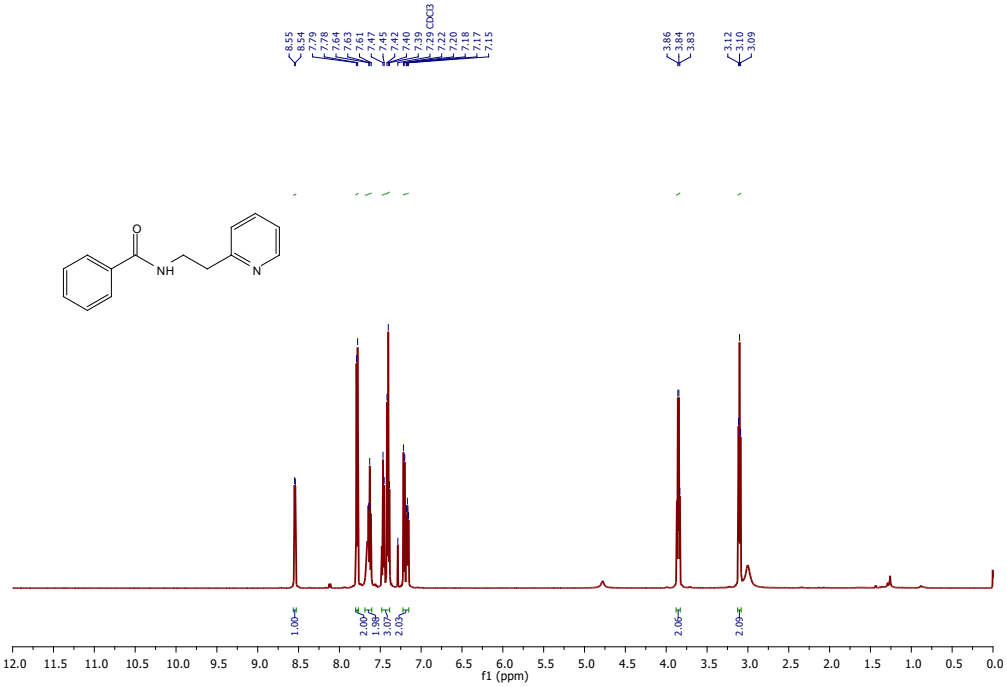

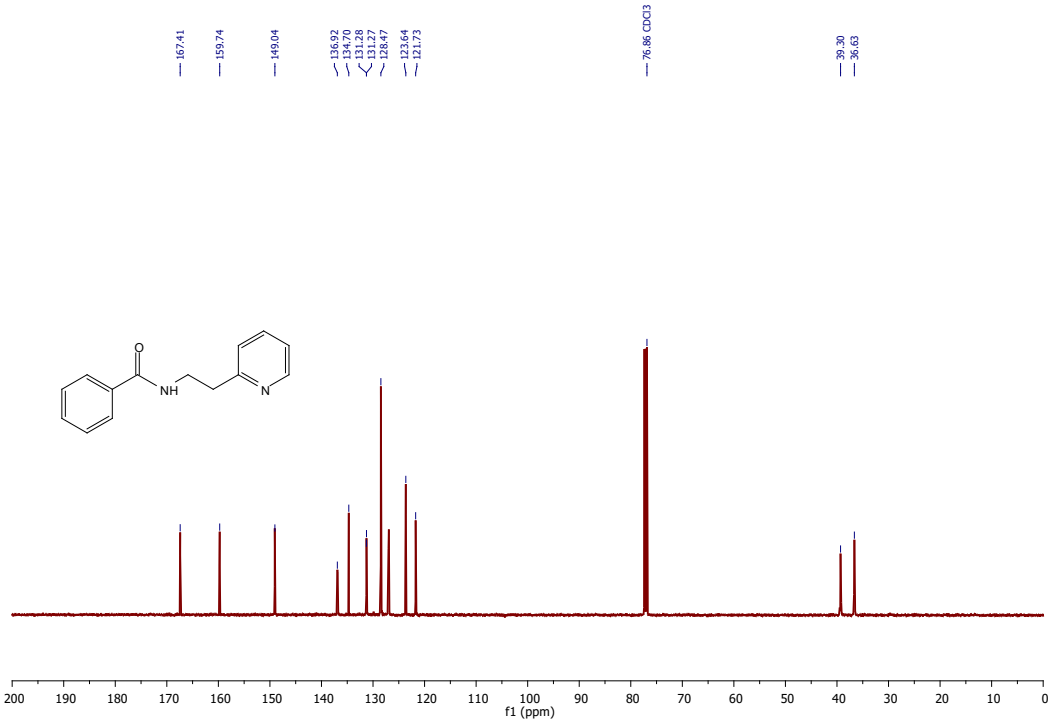

^{1}H and ^{13}C NMR spectra of **3y**

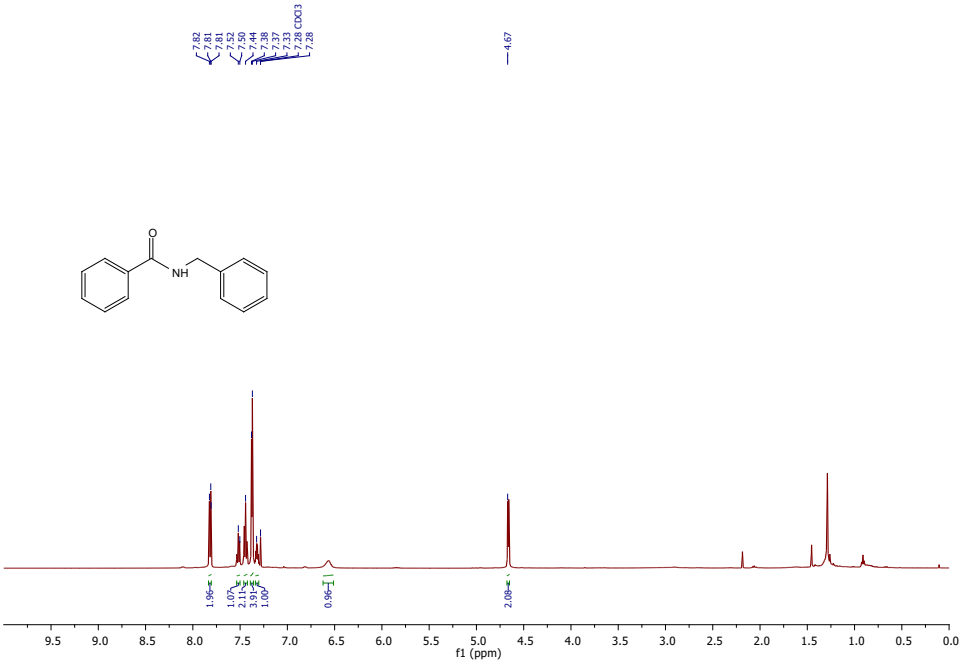

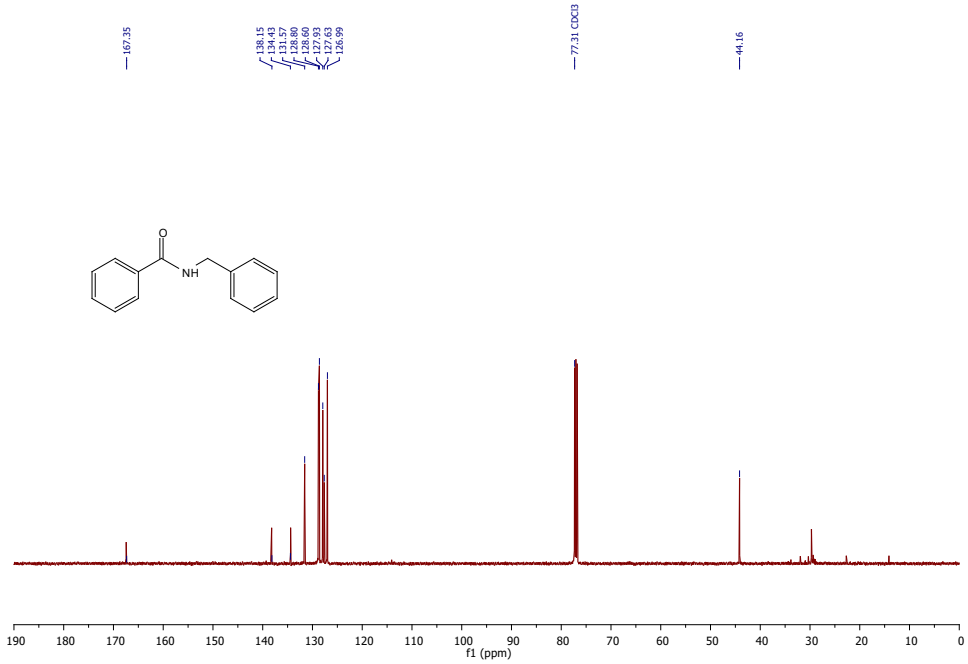

^{1}H and ^{13}C NMR spectra of **3z**

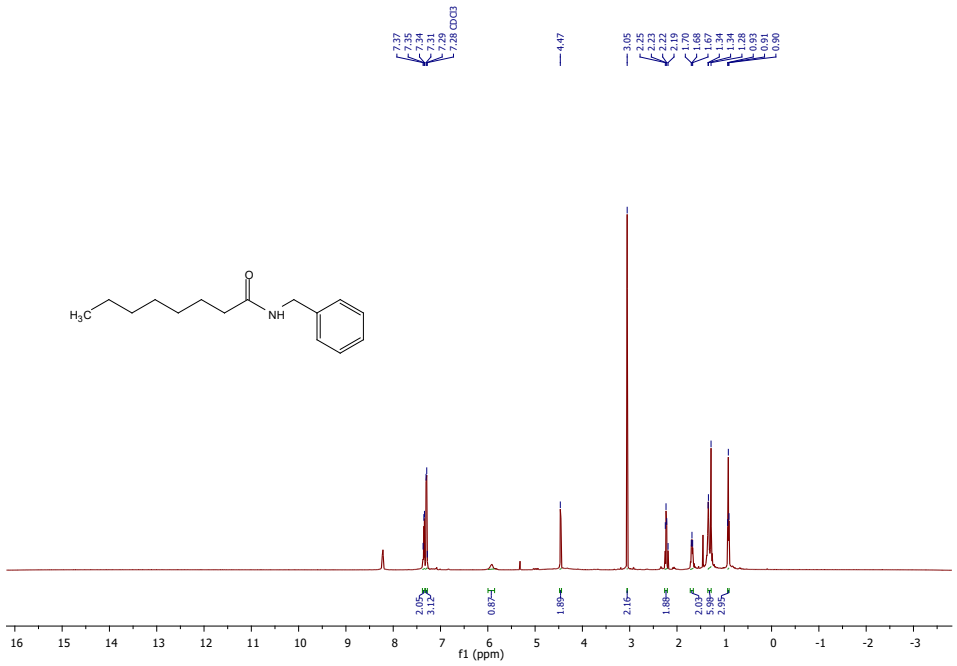

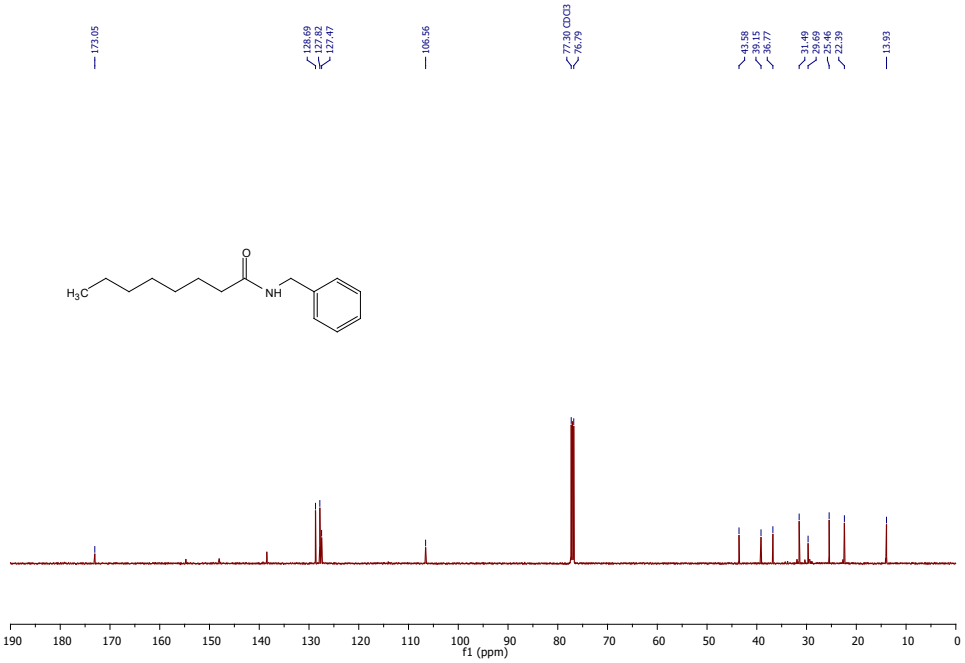

^{1}H and ^{13}C NMR spectra of 3**z′** for HAT mechanism by product.

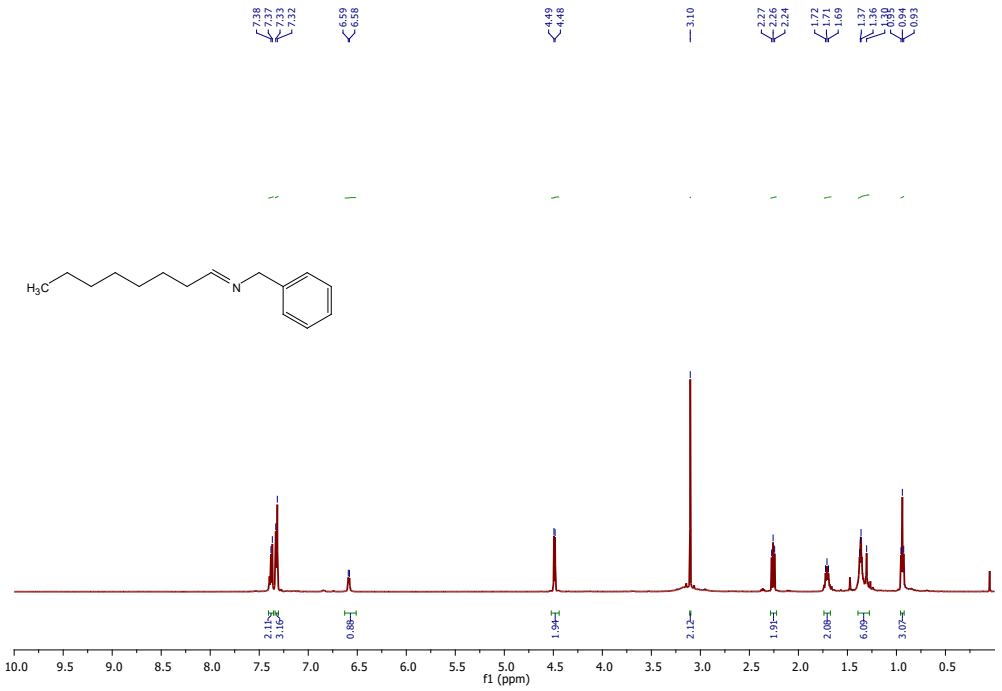

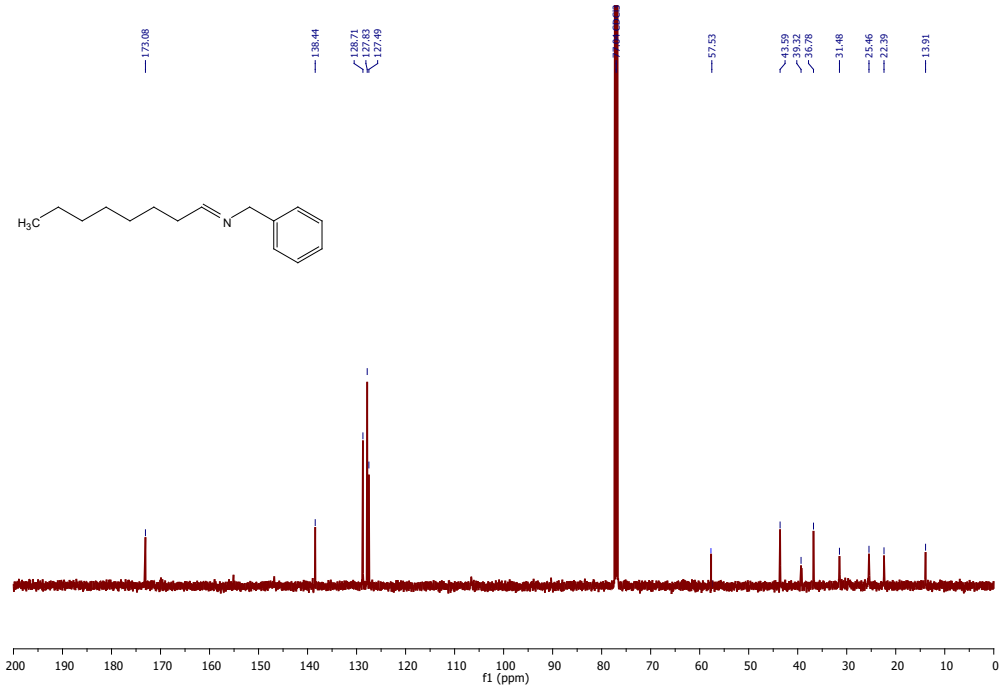

^{1}H and ^{13}C NMR spectra of **3aa**

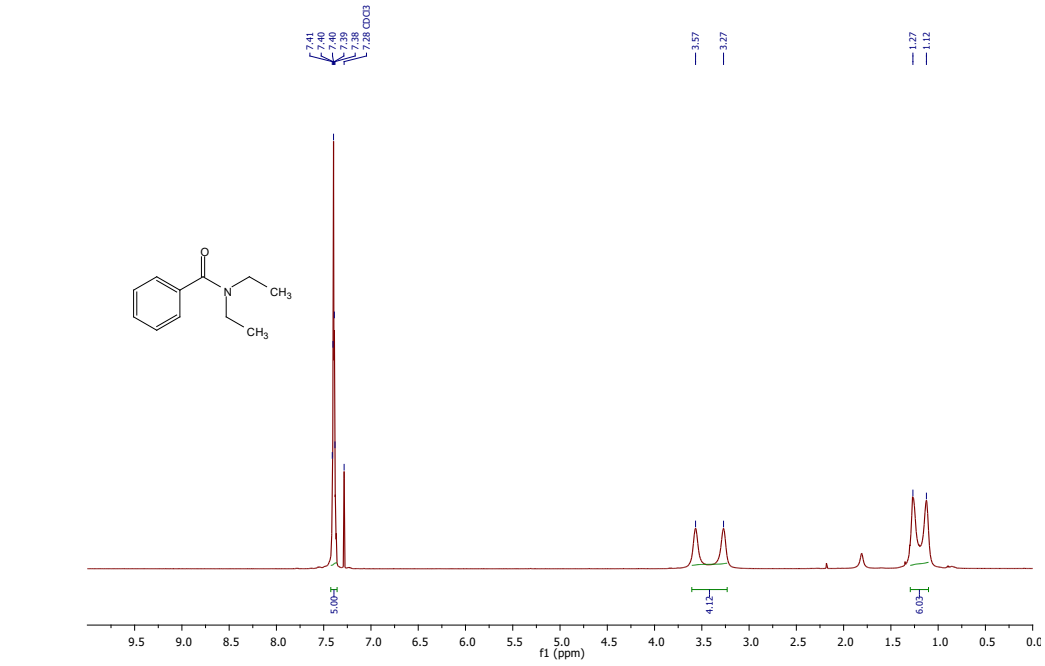

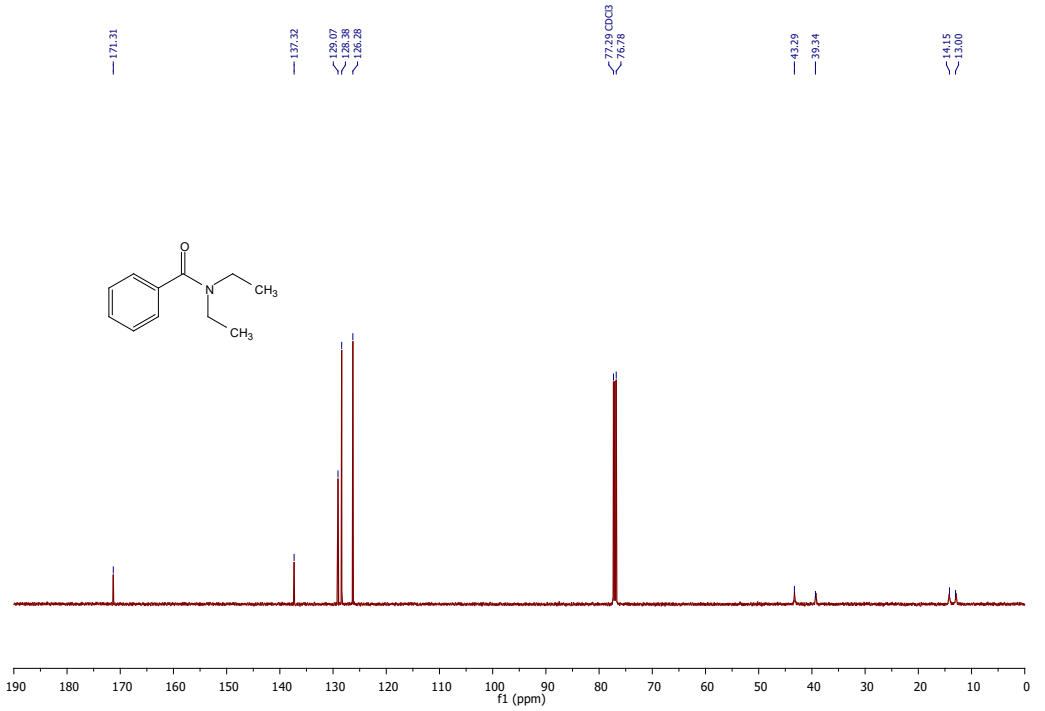

^{1}H and ^{13}C NMR spectra of **3bb**

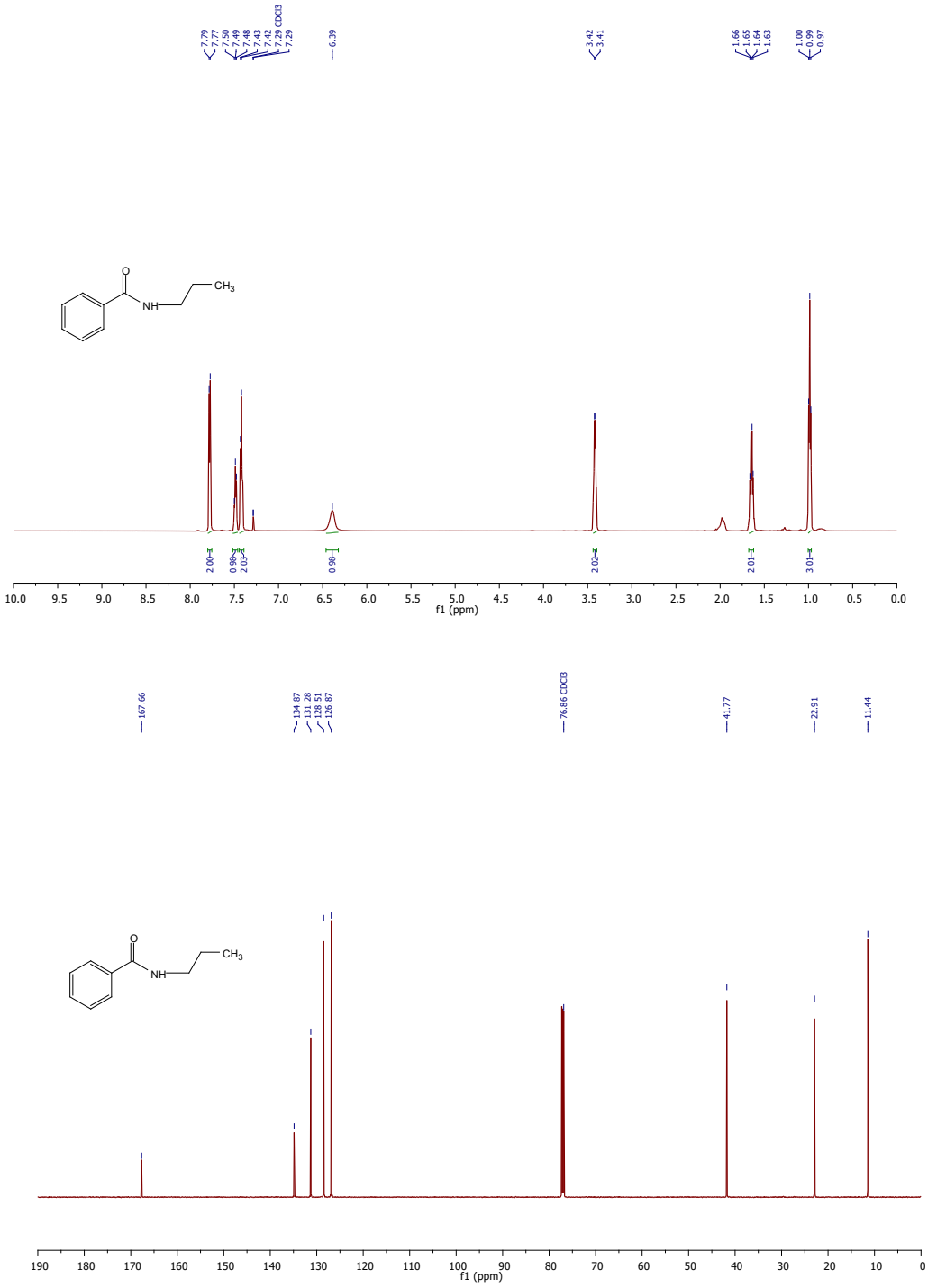

Reference:

1 J. Ding, X. Deng, J. Fan, Y. Wang, Z. Li and Q. Liang, *Inorg. Chem.*, 2023, **62**, 16493–16502.

2 S. Liu, F. Li, T. Li and W. Cao, *J. Colloid Interface Sci.*, 2023, **642**, 100–111.

3 O. C. Compton and F. E. Osterloh, *J. Phys. Chem. C*, 2009, **113**, 479–485.

4 Q. Wang, J. Li, Y. Bai, J. Lian, H. Huang, Z. Li, Z. Lei and W. Shangguan, *Green Chem.*, 2014, **16**, 2728–2735.

5 M. Mohammadikish, *CrystEngComm*, 2014, **16**, 8020–8026.

6 L. Magerusan, C. Socaci, F. Pogacean, M. C. Rosu, A. R. Biris, M. Coros, A. Turza, V. Floare-Avram, G. Katona and S. Pruneanu, *RSC Adv.*, 2016, **6**, 79497–79506.

7 H. Jiang, H. Cheng, C. Zang, J. Tan, B. Sun and F. Bian, *J. Catal.*, 2021, **401**, 279–287.

8 X. Y. L.Wang, M. Yu, C. Wu, N. Deng and C. Wang, *Adv.Synth. Catal* ., 2016, 358, 2631 –2641.

9 L. Xu, S. Z. Zhang, W. Li and Z. H. Zhang, *Chem. - A Eur. J.*, 2021, **27**, 5483–5491.

10 V. Vyas, V. Kumar and A. Indra, *Chem. Commun.*, 2024, **60**, 2544–2547.